HOX11 FUNCTION IN MUSCULOSKELETAL DEVELOPMENT AND REPAIR

by

Ilea T. Swinehart

A dissertation submitted in partial fulfillment
of the requirements for the degree of
Doctor of Philosophy
(Cellular and Molecular Biology)
in the University of Michigan
2013

Doctoral Committee:

Associate Professor Deneen M. Wellik, Chair
Professor Renny T. Franceschi
Professor Deborah L. Gumucio
Associate Professor Catherine Elizabeth H. Keegan

To my amazing friends and family

for all of their support over the years.

TABLE OF CONTENTS

LIST OF FIGURES

CHAPTER I

INTRODUCTION

Hox genes are homeodomain-containing transcription factors that were first described in *Drosophila* for their role in patterning the body plan (Figure 1.1A (Lewis, 1963; Lewis, 1978; Lewis, 1985)). Loss-of-function mutations in *Drosophila HomC*/*Hox* genes results in conversion of a body segment in which that *Hox* gene was expressed into the identity of the next most anterior segment (Figure 1.1B (Lewis, 1978)). This is classically referred to as an anterior homeotic transformation. Conversely, gain of *HomC*/*Hox* gene function in segments anterior to normal expression results in posterior homeotic transformations whereby the anterior segments take on phenotypic characteristics normally formed in the more posterior segment (Figure 1.1C (Kaufman et al., 1990; Schneuwly et al., 1987)).

During vertebrate evolution, a series of cis-amplification and trans-duplication events of the *Drosophila* bithorax and antennapedia complexes occurred to produce the mammalian *Hox* complexes (Krumlauf, 1994; Scott, 1992). In mammals, there are 39 *Hox* genes arranged on four chromosomal clusters. These genes have maintained their closely linked, collinear arrangement. Genes within these clusters fall into one of 13 paralogous groups based on sequence similarity and position within the cluster (Figure

Figure 1.1

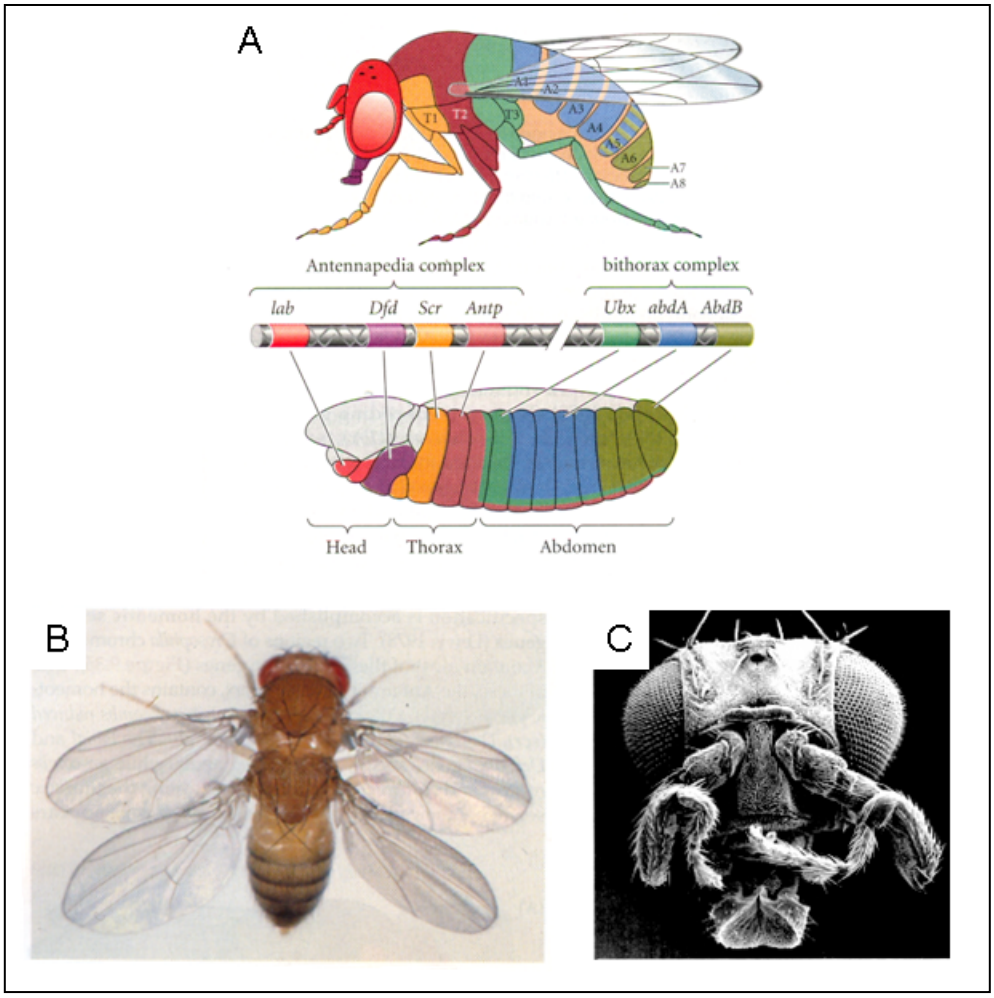

Figure 1.1. Homeotic genes in *Drosophila melanogaster*. Expression of the *HomC* genes along the anterior-posterior body axis (A). Segments of homeotic gene expression in the Drosophila embryo and the segments that form from them in the adult fly are shown. Loss-of-function of *ultrabithorax* results in anterior homeotic transformation of the third thoracic segment (B). Mutants with a gain-of-function of *antennapedia* in the head grow legs instead of antennae, demonstrating a posterior homeotic transformation (C). Images adapted from (Gilbert and Knisely).

Figure 1.2

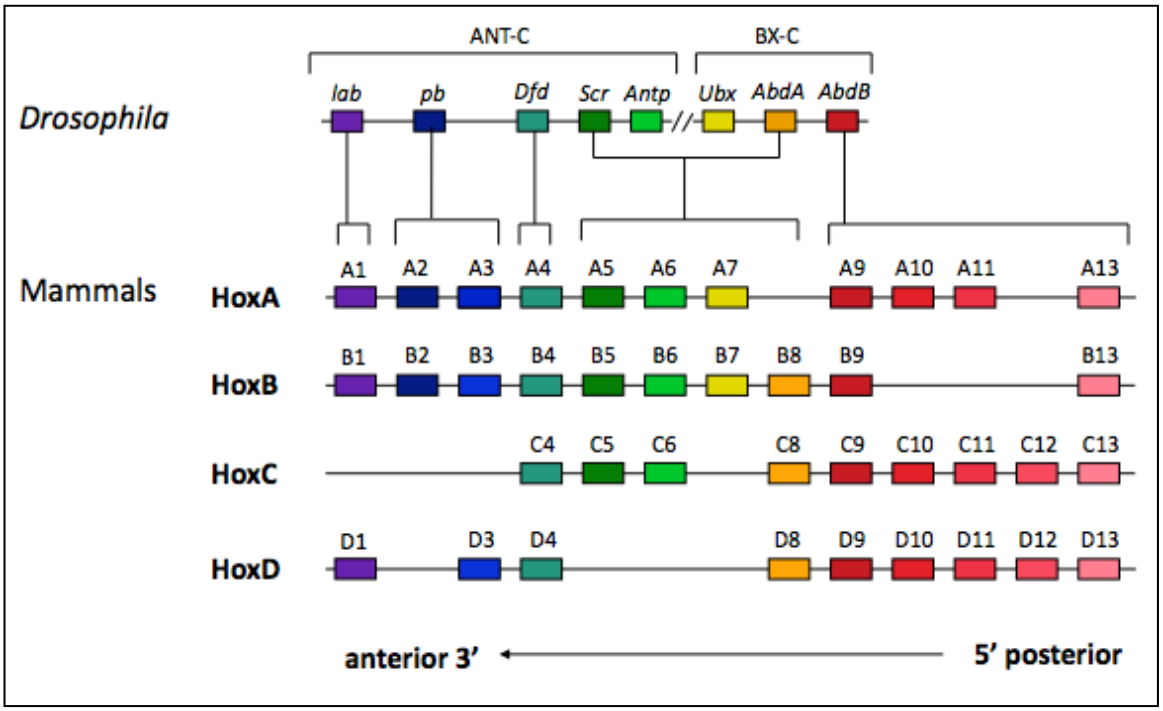

Figure 1.2. Organization of *Drosophila* and mammalian *Hox* genes. Mammals have a total of 39 *Hox* genes arranged on four chromosomal clusters and divided into 13 paralogous groups (genes within a paralogous group are color coded). Members within a paralogous group share a high degree of homology and functional redundancy. Figure adapted from (Wellik, 2007).

1.2) (Pearson et al., 2005). Mammalian *Hox* genes are expressed with spatiotemporal collinearity, with 3' genes being expressed earlier in development and with more anterior limits of expression and 5' genes expressed later and in progressively more posterior domains. Members of each paralogous group share a higher degree of sequence homology with one another than with other genes within the *Hox* cluster. The sequence similarity and similar expression patterns among members of a paralogous group leads to a high degree of functional redundancy. In many cases, when the function of a single *Hox* gene is removed, a mild phenotype is observed due to compensation from other members of the paralogous group. Loss-of-function mutation of multiple paralogous genes or entire *Hox* paralogous groups in mice have consistently resulted in much more dramatic phenotypes (Condie and Capecchi, 1994; Davis et al., 1995; Fromental-Ramain et al., 1996b; Horan et al., 1995; McIntyre et al., 2007; van den Akker et al., 2001; Wellik and Capecchi, 2003; Wellik et al., 2002).

Paralogous *Hox* mutation consistently results in anterior homeotic transformations of the axial skeleton demonstrating that, similar to *Drosophila*, mammalian *Hox* genes function in patterning the body plan and are also critical regulators of skeletal development (Horan et al., 1995; McIntyre et al., 2007; van den Akker et al., 2001; Wellik and Capecchi, 2003). *Hox4* triple mutants show transformation of the second cervical vertebra (C2) through C5 to a C1 phenotype (Horan et al., 1995). *Hox5* triple mutants show transformation of C3 through the first thoracic (T1) vertebra to a C2 phenotype. *Hox6* paralogous mutants display anterior transformation of C6 through T6 (McIntyre et al., 2007). *Hox8* paralogous mutation affects the lower thoracic and lumbar vertebrae (van den Akker et al., 2001). The posterior thoracic vertebrae of *Hox9*

quadruple mutants are transformed such that 13 or 14 ribbed vertebrae make attachment to the sternum instead of the normal complement of 7; several anterior lumbar vertebrae are additionally transformed to ribbed, thoracic morphology (McIntyre et al., 2007). In *Hox10* triple mutants, lumbar and sacral vertebrae are anteriorly-transformed to posterior thoracic vertebrae with rib projections formed throughout lumbosacral regions (Wellik and Capecchi, 2003). *Hox11* triple mutants exhibit transformations of sacral and early caudal vertebrae to a lumbar-like phenotype (Wellik and Capecchi, 2003). There is significant overlap in the regions that exhibit phenotypes between adjacent paralogous groups. Within these overlapping regions, the effect of loss of *Hox* paralogous function is distinct, indicating that each set of paralogs directs specific identities in regions of the axial skeleton.

Hox **genes and patterning in the limb**

Abdominal-B group genes have been co-opted to function in patterning the proximal-distal axis of the developing limb. Similar to the axial skeleton, the limb can be divided into segmental units: the stylopod or humerus/femus, the zeugopod or radius and ulna/tibia and fibula, and the autopod or hand/foot (Figure 1.3). However, unlike the axial regions, loss-of-function mutations of paralogous Hox groups in the limb cannot be interpreted as classical homeotic transformations. Instead, mutation of Abd-B class *Hox* genes in paralogous groups 9-13 results in dramatic mispatterning of skeletal elements within specific limb regions while other regions of the limb are unaffected. *Hox9* and *Hox10* genes function in the stylopod (Fromental-Ramain et al., 1996a; Wellik and Capecchi, 2003), *Hox11* genes function in the zeugopod (Boulet and Capecchi, 2004;

Figure 1.3

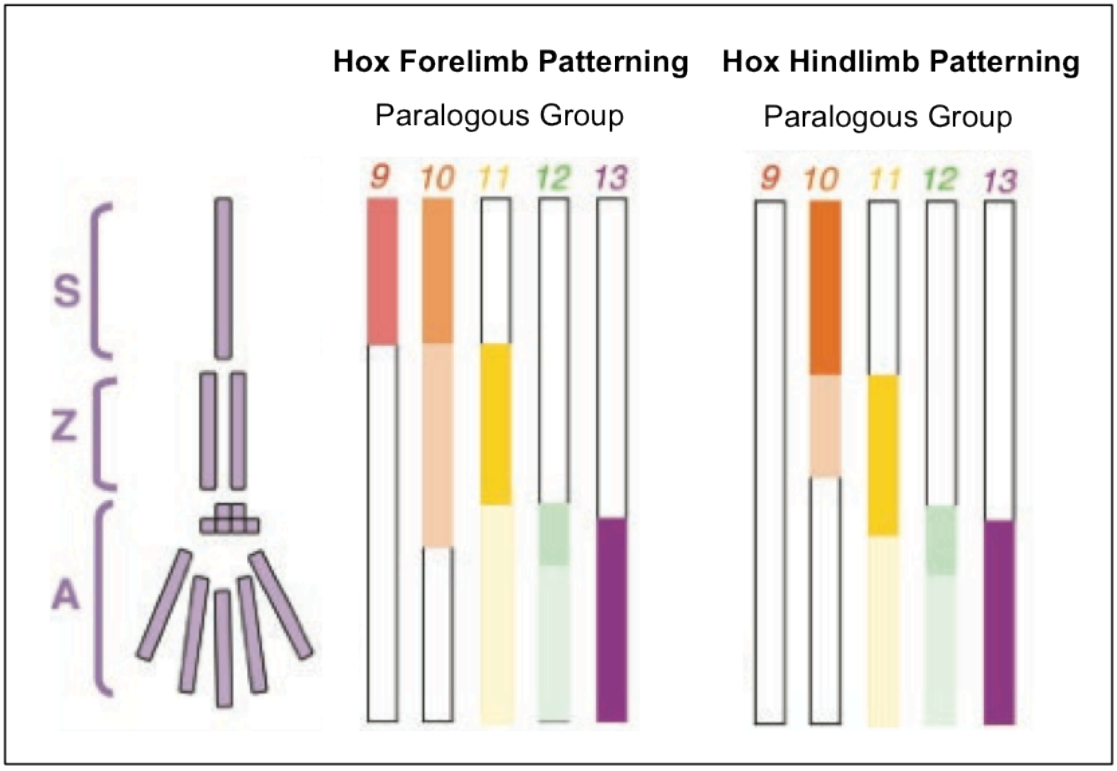

Figure 1.3. *Hox* paralogous groups 9-13 pattern specific limb regions. The functional domains of the AbdB Hox genes in forelimb and hindlimb patterning are diagramed. *Hox9* and *Hox10* paralogous genes function together to pattern the forelimb stylopod. In the hindlimb, *Hox9* paralogs do not function. *Hox11* paralogs function predominantly in zeugopod patterning. *Hox13* paralogs pattern the developing autopod. Lighter shading indicates a lesser contribution of those paralogs in other regions. S denotes stylopod, Z zeugopod, A autopod. Figure adapted from (Wellik and Capecchi, 2003).

Davis et al., 1995; Wellik and Capecchi, 2003) and *Hox13* genes are required for autopod development (Fromental-Ramain et al., 1996b) (Figure 1.3).

Additionally, it was recently shown that *Hox5* and *Hox9* group genes function in non-classical roles in early forelimb patterning. *Hox9* quadruple mutants exhibit severe forelimb defects with complete loss of all posterior skeletal elements (Xu and Wellik, 2011). The defects in *Hox9* mutants result from the loss of *Hand2* expression in the posterior limb bud, which is critical for the initiation of *Shh* signaling. *Hox5* genes are also required for anterior-posterior patterning of the limb. The *Hox9* paralogous mutants phenocopy both *Hand2* and *Shh* loss-of-function mutants, demonstrating its key role in this pathway. Deletion of all three members of the *Hox5* paralogous group results in anterior limb defects as a result of anteriorized *Shh* expression (Xu et al., submitted).

In this thesis, *Hoxa11/d11* double mutants provide a useful model to study the role of *Hox* genes in limb development because inactivation of only two genes is required to disrupt formation of the forelimb zeugopod (Figure 1.4A-B (Boulet and Capecchi, 2004; Davis et al., 1995)). Loss of *Hox11* function does not affect the specification of cartilage condensations but is necessary for proper proliferation, growth and maturation of the chondrocytes (Boulet and Capecchi, 2004). *Hox11* genes are essential for directing the appropriate pattern or morphology of the zeugopod cartilage elements. Other studies of loss of *Hox* function in the limb have suggested potential roles for *Hox* in modulating the rate or timing of cartilage formation, cell adhesion, and chondrogenic capacity (Dollé et al., 1993; Stadler et al., 2001). However, to date, the mechanism of how *Hox* genes pattern skeletal elements is unknown.

Figure 1.4

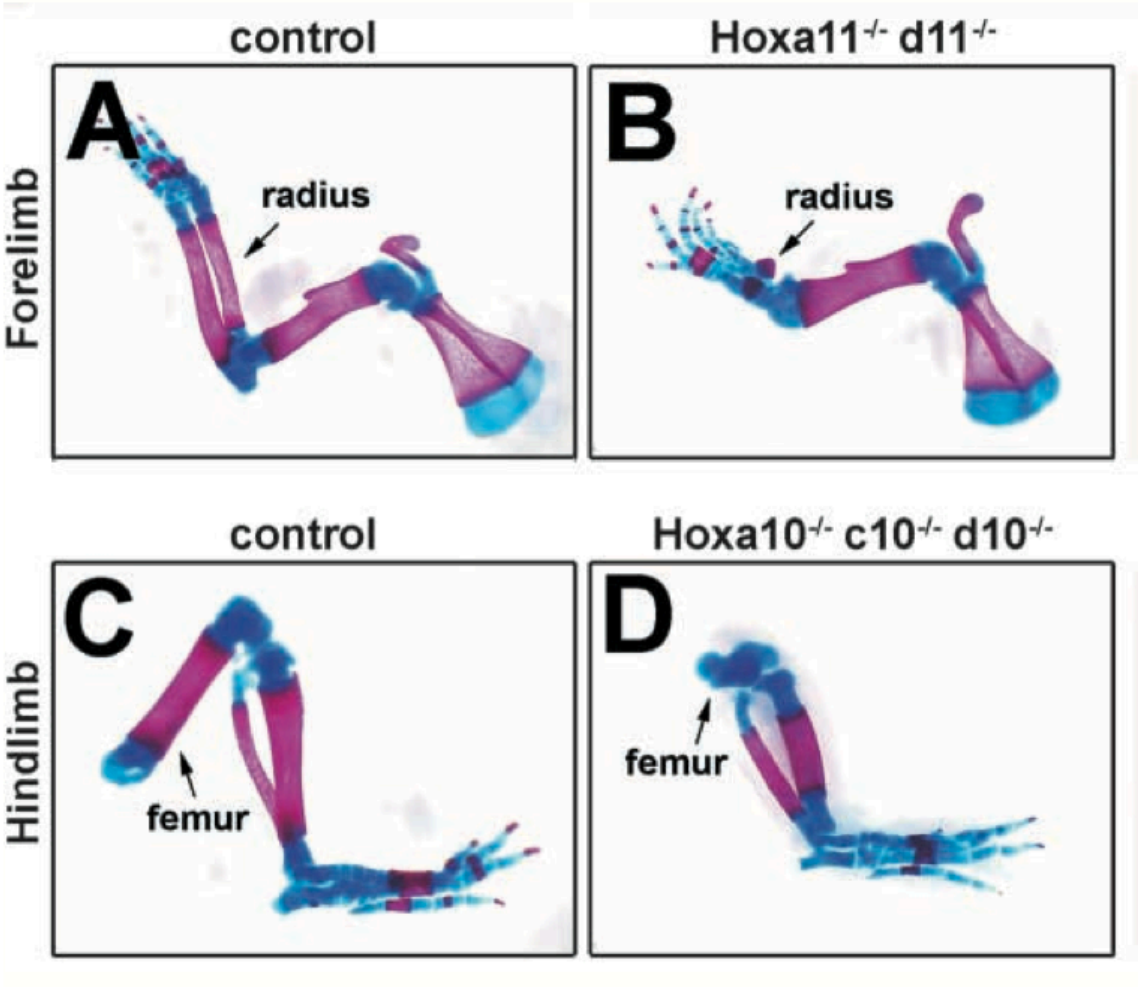

Figure 1.4. Mutation of *Hox* paralogous genes causes truncation of skeletal elements. Forelimbs of (A) control and (B) *Hox11* double mutant newborns stained with alcian blue and alizarin red. Hindlimbs of (C) control and (D) *Hox10* triple mutant newborns. Truncation of zeugopod skeletal elements is observed in *Hox11* mutants and truncation of the stylopod is observed in *Hox10* mutants. Figure adapted from (Boulet and Capecchi, 2004).

Unanswered questions in the field

Genetic analysis of *Hox* mutant skeletal phenotypes has provided insight into the role these genes play in skeletal patterning; however, many questions remain. What downstream transcriptional targets and cellular processes do *Hox* genes regulate? How are these events controlled? These are major questions currently being addressed in our laboratory. In addition, there are other aspects of musculoskeletal patterning in which the role of *Hox* genes has not yet been investigated. Do *Hox* genes provide regional patterning information to other parts of the musculoskeletal system? In mice, examination of *Hox* function in axial and limb patterning has focused primarily on the skeletal phenotypes of *Hox* mutants. This is likely due to the relative ease of analysis of skeletal tissues. However, the expression patterns of *Hox* genes in both the axial regions and limbs are not confined to skeletal tissues, suggesting a potentially broader role for *Hox* genes in patterning of the musculoskeletal system. Our understanding of the cell types in which *Hox* genes function and the tissues they pattern is incomplete.

A possible role for *Hox* genes in postnatal growth and/or skeletal repair has also not been previously examined. *Hox* genes are expressed throughout development and expression continues into postnatal and adult stages in the periosteum. The repair of skeletal fractures is a regenerative process that recapitulates many mechanisms of the initial skeletal development and growth. As during embryogenesis, fracture repair is dependent on instructional cues from the local environment. *Hox* genes may provide regional patterning information during postnatal growth and adult repair analogous to their role during initial skeletal development.

The objective of this thesis research was to examine the function of *Hox11* genes in musculoskeletal patterning, postnatal growth, and fracture repair. Our ultimate goal is to elucidate the cellular and molecular mechanisms by which *Hox* genes determine morphology.

Establishment of the musculoskeletal pattern

The musculoskeletal pattern of the vertebrate limb is highly complex with more than 40 muscles connected through tendons to the limb skeleton. Precise coordination of muscle, tendon, and cartilage formation, and the integration of these tissues during development is necessary to create a functional system that is capable of both a large range of movement and fine motor control. Studies using chick as a model organism have demonstrated that the limb musculoskeletal system is derived from two mesodermal cell populations (Chevallier et al., 1977; Christ et al., 1977b). Muscles derive from the lateral dermomyotome of somites medial to the limb bud, while tendon and cartilage derive directly from the lateral plate mesoderm within the limb bud. Somitic myogenic precursors migrate into the limb bud where they then proliferate, aggregate and differentiate to form dorsal and ventral muscle masses (Chevallier et al., 1977; Christ et al., 1977b; Ordahl and Le Douarin, 1992; Wachtler et al., 1981). These muscle masses then segregate into individual, anatomically distinct muscle masses. Concurrently, cartilage precursors condense within the limb bud mesoderm to produce the skeletal anlage. Additionally, tendon primordia arise from within the limb mesoderm in dorsal and ventral areas of the limb and subsequently align between the muscle masses and skeletal elements (Schweitzer et al., 2001).

Subsequent tendon morphogenesis requires the presence of muscles, as tendon progenitors are progressively lost from proximal to distal regions in the absence of muscle invasion (Bonnin et al., 2005; Edom-Vovard et al., 2002; Eloy-Trinquet et al., 2009; Kardon, 1998; Kieny and Chevallier, 1979). Surgical manipulation experiments demonstrate the reciprocal interactions between muscle and tendon during development. Removal of the tendon primorida results in aberrant muscle formation demonstrating a role for tendon in negatively regulating muscle development within specific limb regions (Kardon, 1998). Muscle and tendon are also necessary for patterning the secondary characteristics of the skeleton. It has long been known that the formation of bone ridges depends on mechanical forces provided by muscle (Hall and Herring, 1990; Hosseini and Hogg, 1991). More recent evidence demonstrates that bone ridge formation is a biphasic process that is first initiated by signaling from the tendon (Blitz et al., 2009). It is important to consider that these tissues do not develop in spatial isolation but are interconnected and coordinated throughout embryogenesis.

While the molecular pathways that determine muscle and cartilage cell fate are well understood, very little is known about the mechanisms that regulate the morphogenesis of individual muscles or their associated tendons and skeletal attachments. Embryologic manipulation experiments have shown that muscles do not posses intrinsic regulatory information to establish their own pattern. In experiments where somites from an axial level outside the normal limb region are transplanted to replace limb somites, the muscle cells migrate into the limb and are able to give rise to normal limb muscle (Chevallier et al., 1977; Christ et al., 1977b). In addition, classical chick-quail graft experiments and single-cell lineage analysis of muscle precursors

reveals that individual myogenic cells are not predetermined to form any particular anatomical muscle (Chevallier et al., 1977; Christ et al., 1977b; Christ et al., 1977a; Kardon et al., 2002). Therefore, muscle patterning information must be provided by other cells within the limb mesenchyme after muscle cells have migrated into the limb (Jacob et al., 1979). Experiments with muscle-less limbs have shown that muscle connective tissue (MCT), the connective tissue within and ensheathing the muscle, is patterned in the absence of muscle invasion and is capable of patterning non-muscle cells, leading to the idea that MCT regulates the patterning of migrating myoblasts (Chevallier and Kieny, 1982; Grim and Wachtler, 1991). More recently, the transcription factor Tcf4, a member of the Tcf/Lef family that acts downstream of Wnt signaling, has been identified as a marker of MCT (Kardon et al., 2003). *Tcf4* mutant mice display reduced limb mobility and muscle mispatterning (Kardon et al., 2003; Mathew et al., 2011). The T-box transcription factors Tbx4 and Tbx5 are also expressed within the limb mesenchyme, including the MCT, and *Tbx5* deletion leads to mispatterning and ectopic splitting of limb muscles (Hasson et al., 2010). The MCT of *Tbx5* mutants is highly disorganized and β-Catenin and N-cadherin are reduced in these animals. These experiments suggest that β-Catenin mediated cell adhesion plays an essential role in MCT organization and that the organization of MCT is critical for its patterning activities.

Muscle connective tissue is one of several tissues that have been implicated in regulating the process of muscle splitting. The nervous system was initially proposed to direct the splitting process; however, this has been disproven by experiments that show that limb muscles split normally in the complete absence of innervation (Edom-Vovard et

al., 2002; Rong et al., 1992). In the chick autopod, retinoic acid signaling has been shown to regulate apoptosis within the muscle masses, thereby resulting in cleavage (Rodriguez-Guzman et al., 2007). An association has also been made between the splitting site and vasculature development. Using overexpression assays, it was shown that platelet derived growth factor-B (PDGF-B), secreted from endothelial cells, participates in muscle splitting by causing an upregulation of extracellular matrix and connective tissue markers including *Tcf4* (Tozer et al., 2007). It is likely that some combination of these processes directs muscle cleavage events by promoting connective tissue formation or differentiation within the muscle mass. Muscle patterning defects observed with the deletion of genes expressed within the MCT, such as *Tcf4* and *Tbx4*/5 lends support to the idea that MCT contributes to muscle splitting; however, the mechanisms by which MCT establishes a prepattern for muscle and regulates muscle splitting are not understood.

Skeletal repair

It is estimated that approximately 7.9 million skeletal fractures occur in the U.S. each year (Axelrad et al., 2007). Depending on the type of fracture and the location of the injury, it can take from 4-13 months to achieve healing (Drosos and Pozo, 2005; Oni et al., 1988). Approximately 10% of fractures result in impaired or delayed healing. This has a significant impact on both the quality of life for the patient and greatly increases the medical costs associated with treatment. It is estimated that each tibial non-union has a direct cost of approximately $7,500 (Busse et al., 2005). An improved understanding of

the complex biological pathways that are initiated during the fracture healing response will increase our ability to treat delayed healing and non-union after fracture.

The repair of skeletal fractures is a regenerative process that recapitulates many of the mechanisms of initial skeletal development (Ferguson et al., 1999; Vortkamp et al., 1998). As with embryological patterning and skeletal growth, fracture healing relies on patterning cues from the local environment. However, the postnatal and adult tissue environment in which the fracture repair process occurs is different in several respects compared to that present during development.

Fracture healing where there is motion at the injury site occurs through the formation of a large cartilage scaffold that is gradually replaced by bone that then undergoes extensive remodeling to establish the original skeletal morphology. This type of healing recapitulates some of the steps involved in embryonic endochondral ossification. Intramembranous ossification, in which mineralized tissue is formed directly without the creation of a cartilage template, also contributes to fracture repair. This is dissimilar to development where intramembranous ossification only occurs in the flat bones of the skull.

The fracture repair process occurs in four consecutive but overlapping stages: 1.) the inflammatory response, 2.) soft callus formation, 3.) hard callus formation, and 4.) bone remodeling (Figure 1.5). This four-stage model is based on histological observations of healing fractures. The cellular and molecular mechanisms that drive the regenerative process are still under active investigation.

The initial inflammatory phase of fracture healing is distinct from developmental bone formation. This process is associated with a disruption of the local soft tissue,

vasculature, and marrow architecture. During this phase, there is bleeding within the fracture site into the surrounding tissue and a local hematoma develops (Figure 1.5A). Many inflammatory cells localize to the fracture site, including macrophages, granulocytes, lymphocytes and monocytes. These cells combat infection and secrete cytokines and growth factors, including transforming growth factor-β (TGF-β), platelet-derived growth factor (PDGF), fibroblast growth factor 2 (FGF2), and vascular endothelial growth factor (VEGF) (Bolander, 1992; Gerstenfeld et al., 2003).

In response to growth factors released by inflammatory cells and neighboring cells and tissues, mesenchymal cells actively populate the wound site where they proliferate and differentiate to form a cartilaginous soft callus (Figure 1.5B (Bolander, 1992; Bruder et al., 1994)). During this second stage, the callus is dominated by chondrocytes and fibroblasts. Chondrocyte maturation and vascular invasion during this stage follows similar molecular programs as during embryonic skeletal development (Ferguson et al., 1999).

The third stage, hard callus formation, is characterized by the formation of osteoblast mediated mineralized bone matrix formation, beginning in peripheral areas of the callus (Figure 1.5C). High levels of associated angiogenesis during this stage of healing is critical for fracture repair (Hankenson et al., 2011). Osteoblast progenitors migrate into the callus along with invading blood vessels (Maes et al., 2010). The initial woven bone matrix is a combination of proteinaceous and mineralized extracellular matrix tissue and is highly irregular and disorganized compared to the original bone prior to fracture.

Figure 1.5

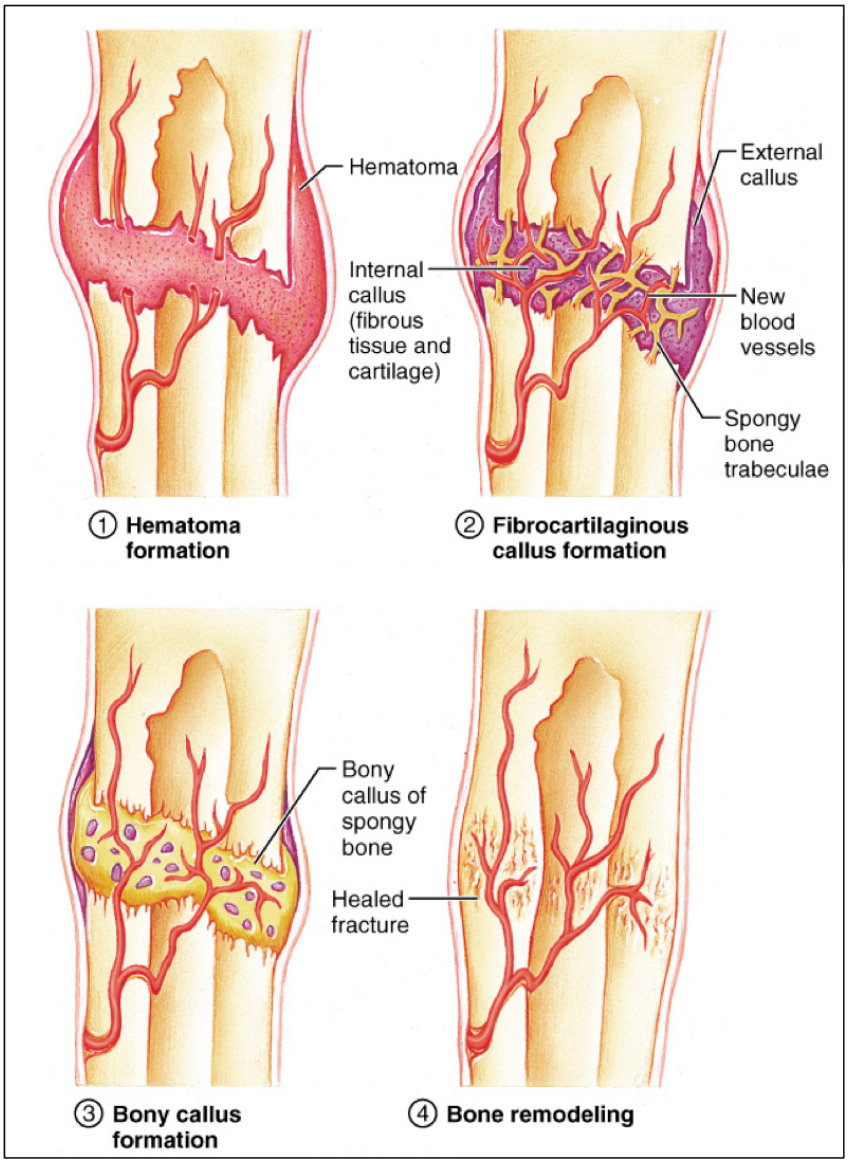

Figure 1.5. Stages of fracture repair. Fracture healing occurs in four main stages: 1. Inflammatory cells infiltrate the injury site and secrete cytokines and growth factors. 2. A soft, cartilage based callus is formed to stabilize the fracture. 3. A hard callus of mineralized bone matrix is produced by osteoblasts. 4. The callus is remodeled into cortical bone by osteoclasts. Figure adapted from Pearson Education.

In the fourth and final stage, the woven bone hard callus undergoes extensive remodeling to re-establish the original cortical and/or trabecular bone morphology (Figure 1.5D). This remodeling is carried out largely by osteoclasts. The osteoclast is a large, multinucleated cell formed by the fusion of mononucleate precursors of the monocyte/macrophage lineage (Väänänen and Laitala-Leinonen, 2008). Osteoclasts degrade the mineralized matrix by targeted secretion of acid and proteinases. Bone resorption is coupled to formation of lamellar bone to complete the remodeling process. How cells in this region are instructed to return to normal morphology is not understood.

The source of progenitor cells that give rise to formation of the callus is very poorly understood and of considerable interest. Several potential sources of cells for this regenerative process have been implicated including the periosteum (Malizos and Papatheodorou, 2005; Nakahara et al., 1990), bone marrow (Baksh et al., 2004; Colnot et al., 2006; Mehrotra et al., 2012), systemically circulating cells (Khosla and Eghbali-Fatourechi, 2006; Matsumoto et al., 2008), surrounding soft tissues (Henrotin, 2011; Rumi et al., 2005), and perivascular cells (Maes et al., 2010). Mesenchymal stem cells (MSCs) are of particularly high interest for us in fracture repair treatments and there is a considerable need for novel approaches to improve fracture healing and treat fracture non-unions and bone defects (Jones and Yang, 2011; Khosla et al., 2010; Park et al., 2012). However, the role of MSCs and other cells in the repair process is not understood. Defining the cell populations that contribute to callus formation and repair will inform stem cell based therapies for skeletal repair and replacement strategies.

Recent evidence suggests that *Hox* expression is maintained throughout adult life in multiple tissue types, including skeletal tissues (Ackema and Charité, 2008; Chi et al.,

2007; Gesta et al., 2006; Leucht et al., 2008; Rinn et al., 2006; Rinn et al., 2008). These studies show that at least some aspects of regionally restricted *Hox* expression domains are maintained into adult life. During embryogenesis, *Hox* genes provide critical regional patterning cues to the developing skeleton that are necessary for growth plate establishment and chondrocyte maturation. While the function of *Hox* genes in skeletal repair is not understood, the molecular mechanisms of fracture healing are very similar to skeletal development (Ferguson et al., 1999). One question addressed in this thesis is whether *Hox* genes may be reactivated during repair (Gersch et al., 2005) and could provide regional patterning information to guide the regenerative process.

CHAPTER II

HOX11 FUNCTION IS REQUIRED FOR REGIONAL PATTERNING AND INTEGRATION OF MUSCLE, TENDON AND BONE

SUMMARY

Development of the musculoskeletal system requires precise integration of muscles, tendons and bones. The molecular mechanisms involved in the differentiation of each of these tissues have been the focus of significant research; however, much less is known about how these tissues are integrated into a functional unit appropriate for each body position and role. Previous reports have demonstrated critical roles for *Hox* genes in patterning the axial and limb skeleton. Loss of *Hox11* paralogous gene function results in dramatic malformation of limb zeugopod skeletal elements, the radius/ulna and tibia/fibula, as well as transformation of the sacral region to a lumbar phenotype. Utilizing a *Hoxa11eGFP* knock-in allele, we show that *Hox11* is expressed in the connective tissue fibroblasts of the outer perichondrium, tendons and muscle connective tissue of the zeugopod region throughout all stages of development. *Hox11* is not expressed in differentiated cartilage or bone, or in vascular or muscle cells in these regions. Loss of *Hox11* function disrupts regional muscle and tendon patterning of the limb in addition to affecting skeletal patterning. The tendon and muscle defects in *Hox11* mutants are independent of skeletal patterning events as disruption of tendon and muscle

patterning is observed in *Hox11* compound mutants that do not have a skeletal phenotype. Thus, *Hox* genes are not simply regulators of skeletal morphology as previously appreciated, but are key factors that regulate regional patterning and integration of the musculoskeletal system.

INTRODUCTION

The vertebrate limb provides a powerful system for the study of tissue patterning and morphogenesis. The vertebrate limb musculoskeletal system is a highly complex structure with over 40 distinct muscles connected through tendons to skeletal elements. The morphology of each individual muscle and bone is designed to perform a specific function in order to generate a large range of movement and fine motor control of the limb. These tissues must be precisely patterned and integrated during development to perform properly. Considerable knowledge has been accumulated regarding the molecular pathways involved in the differentiation of each of the tissue types: muscle, tendon, and bone (Buckingham et al., 2003; Karsenty et al., 2009; Tozer and Duprez, 2005). However, much less is known about how the tissues are properly integrated with one another to produce functional units for locomotion.

Hox genes have been long appreciated to provide important patterning cues along the anterior-posterior axis of the vertebral skeleton and the proximal-distal axis of the limb skeleton (Izpisúa-Belmonte and Duboule, 1992; Mallo et al., 2010; Wellik, 2007). There is a high degree of sequence similarity and functional redundancy between members within a *Hox* paralogous group (Mallo et al., 2009; Wellik, 2007). Loss-of-function of Abdominal-B class *Hox* genes from paralogous groups 9-13 results in

disrupted patterning of limb skeletal elements within specific proximal-distal regions while other regions of the limb are largely unaffected. *Hox9* and *Hox10* paralogous genes pattern the stylopod skeleton (femur or humerus) (Fromental-Ramain et al., 1996a; Wellik and Capecchi, 2003), *Hox11* genes function in the zeugopod (radius/ulna, tibia/fibula) (Boulet and Capecchi, 2004; Davis et al., 1995; Wellik and Capecchi, 2003) and *Hox13* genes are required for autopod development (Fromental-Ramain et al., 1996b). During limb morphogenesis, dynamic expression patterns are observed for *Hox* genes. They are first expressed broadly in the distal mesenchyme of the early limb bud and later become restricted along the proximal-distal axis to the regions they pattern, with *Hox9* and *Hox10* genes most proximal and *Hox13* genes most distal (Izpisúa-Belmonte and Duboule, 1992; Nelson et al., 2008; Zakany and Duboule, 2007).

Using a *Hoxa11eGFP* knock-in/knock-out allele to visualize *Hox11* expression and inform possible mechanisms of *Hox* patterning of limb skeletal elements, we found the surprising result that *Hox11* expression is largely excluded from condensing cartilage from the earliest stages. *Hox11* is expressed strongly in the outer perichondrial layer of the developing zeugopod, throughout the tendons, and also in the muscle connective tissue of the forelimb zeugopod. In the absence of *Hoxa11* and *Hoxd11,* muscle and tendon patterning in the forelimb zeugopod is severely disrupted in addition to the previously reported skeletal defects, while musculoskeletal patterning in the stylopod and autopod region is largely unaffected. In *Hox11* mutants, numerous muscles and tendons are absent and others fail to separate into properly patterned muscle bundles. In compound mutants with a single wild-type allele of either *Hoxa11* or *Hoxd11*, the limb skeleton develops normally through embryonic stages, however, muscle and tendon

patterning is disrupted, demonstrating that the tendon and muscle patterning defects are not secondary to perturbation of skeletal morphology. Our finding shifts the paradigm of *Hox* function in musculoskeletal patterning from one where *Hox* genes are critical skeletal patterning factors to one that recognizes their key role in the patterning and integration of all three tissue types of the musculoskeletal system; the bone, tendon and muscle. The expression of *Hox11* genes in the zeugopod suggests *Hox* genes function regionally in connective tissues to control these events throughout development.

RESULTS

Expression of *Hox11* during zeugopod development

Hox11 genes are critical for the morphogenesis of the zeugopod skeletal elements. Loss-of-function of all three members of the *Hox11* paralogous group (*Hoxa11*, *Hoxc11*, and *Hoxd11*) results in dramatic mispatterning of forelimb and hindlimb zeugopod (Wellik and Capecchi, 2003). Because *Hoxc11* is not expressed in the forelimb, inactivation of only two members of the *Hox11* paralogous group, *Hoxa11* and *Hoxd11,* is required to disrupt the formation of the forelimb zeugopod (Figure 2.1A,B (Boulet and Capecchi, 2004; Davis et al., 1995)).

We examined the forelimb expression pattern of *Hoxa11* utilizing a previously described *Hoxa11eGFP* targeted knock-in allele which has been shown to closely recapitulate reported mRNA expression patterns of *Hoxa11* (Haack and Gruss, 1993; Hsieh-Li et al., 1995; Nelson et al., 2008; Small and Potter, 1993). *Hoxa11* and *Hoxd11* display similar expression patterns during forelimb development and *Hoxd11* duplication can compensate for the loss of *Hoxa11* gene function in the zeugopod, further

Figure 2.1

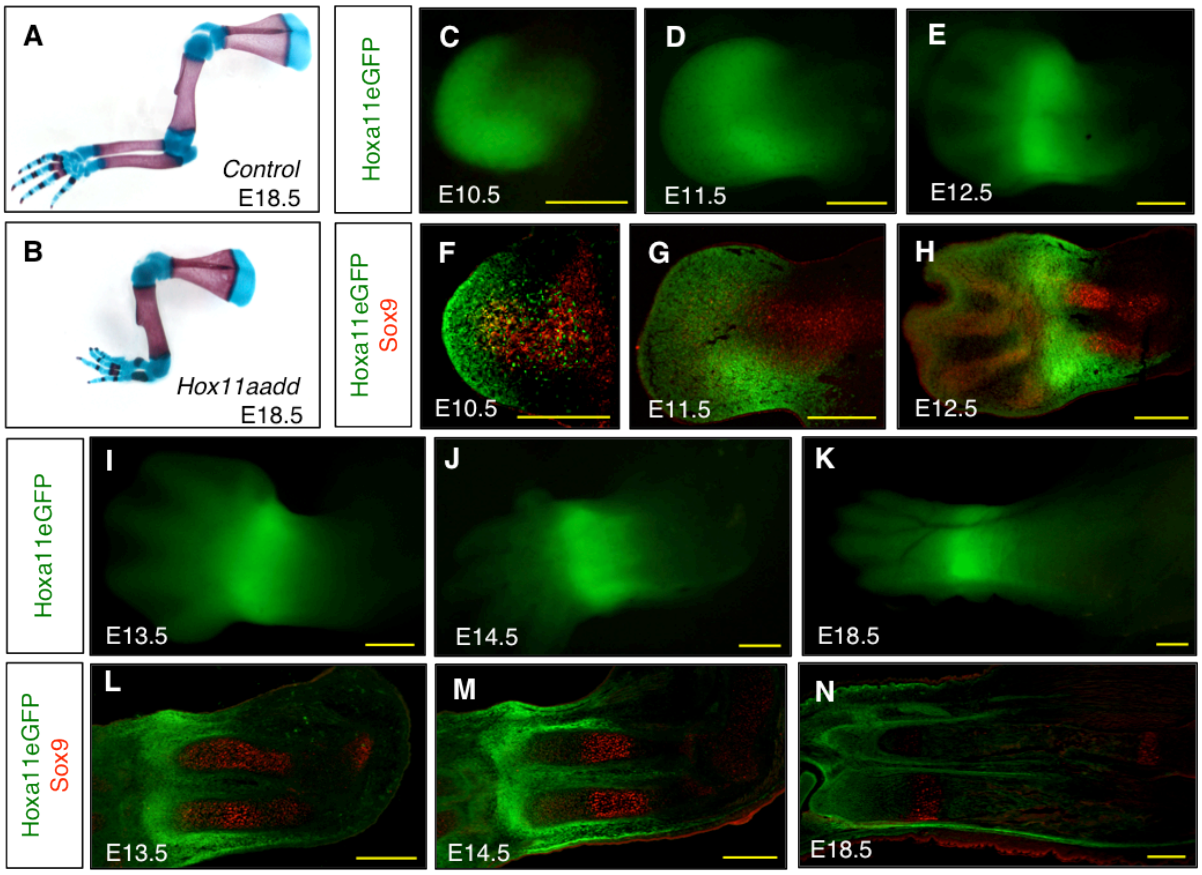

Figure 2.1. Forelimb zeugopod skeletal elements are mispatterned in *Hoxa11/d11* double mutants and *Hoxa11eGFP* expression is maintained in the zeugopod throughout forelimb development. Alcian blue and alizarin red stained skeletal preparations of E18.5 control (A) and *Hoxa11/d11* double mutant (B) forelimbs. Whole mount view of *Hoxa11eGFP* heterozygous embryo forelimb at E10.5 (C), E11.5 (D), E12.5 (E), E13.5 (I), E14.5 (J), and E18.5 (K). Transverse sections through *Hoxa11eGFP* heterozygous forelimb co-stained with an antibody for the pre-chondrogenic marker Sox9 (red) at E10.5 (F), E11.5 (G), E12.5 (H), E13.5 (L), E14.5 (M), E18.5 (N). Yellow bar denotes 300 μm.

demonstrating that spatial, temporal, and functional aspects of *Hoxa11* and *Hoxd11* activity correspond closely in this aspect of limb patterning (Boulet and Capecchi, 2002; Hostikka and Capecchi, 1998). At embryonic day (E) 10.5, whole-mount analysis shows *Hoxa11eGFP* expression is strongest at the distal end of the limb bud with expression extending into the central limb mesenchyme (Figure 2.1C). *Hoxa11eGFP* fluorescence remains relatively ubiquitous in the distal limb bud at E11.5, although a more intense band of expression can be observed in the developing distal zeugopod region (Figure 2.1D). As development proceeds, *Hoxa11eGFP* expression becomes strongest in the zeugopod and is reduced in the autopod (Figure 2.1E,I-K).

Examination of longitudinal sections through E10.5 limb bud reveals that *Hoxa11eGFP* is expressed ubiquitously and uniformly throughout the distal limb bud mesenchyme (Figure 2.1F). Additionally, a subset of cells proximal to the proliferative zone is GFP positive (Figure 2.1F). Co-staining these sections with an antibody for the pre-chondrocyte marker Sox9 demonstrates that Sox9 and *Hox11* expression are largely exclusive. Only a few cells at the distal end of the Sox9 expression domain appear to co-expresses *Hoxa11eGFP*. Most *Hoxa11eGFP* positive cells at this stage are interspersed with the Sox9-expressing cells but are non-overlapping (Figure 2.1F). *Hoxa11eGFP* remains exclusive from the Sox9-expressing cells after condensation of pre-cartilage into the skeletal elements of the zeugopod (Figure 2.1G,H).

By E12.5, the stage at which the two zeugopod skeletal elements are forming distinct anlage, *Hoxa11eGFP* expression is largely restricted to the distal zeugopod region. Within the next 24 hours of development, *Hox11* expression is observed surrounding the zeugopod elements (Figure 2.1H,L). *Hoxa11eGFP* expression is

maintained through the remaining stages of embryonic development, surrounding the radius and ulna with strongest expression distally in these elements (Figure 2.1M,N).

Hoxa11eGFP is expressed in the outer perichondrium, tendons, and muscle connective tissue

The perichondrium/periosteum functions as a signaling center for the underlying chondrocytes (Colnot et al., 2004; Kronenberg, 2007). The periosteum is composed of two layers, an outer layer composed of stromal fibroblasts whose roles are not fully understood but provide the immediate attachment site for tendons and ligaments. The second layer is the inner periosteal, osteoblast-containing layer that contributes directly to appositional growth (Bandyopadhyay et al., 2008; Pathi et al., 1999). Runx2 and Osterix (Osx) are essential transcription factors expressed at early osteoblast differentiation stages in the inner periosteal layer (Komori et al., 1997; Nakashima et al., 2002; Otto et al., 1997). By E13.5, *Hoxa11eGFP* is expressed strongly in the cells of the outer periosteum of the zeugopod but is excluded from chondrocytes as well as the Runx2- and Osx-expressing inner periosteal/osteoblast layer (Figure 2.2A,B). Close examination of Osx and *Hoxa11eGFP* shows that *Hoxa11* is expressed in the cells immediately adjacent to the Runx2/Osx-expressing inner periosteal layer (Figure 2.2B'). *Hoxa11eGFP* is not co-expressed with Runx2 or Osterix at any developmental stage examined. Additionally, *Hoxa11eGFP* does not co-express with the osteoblast reporter Bmp2 ECR LacZ (Chandler et al., 2007), confirming exclusion of expression from the inner periosteal, osteoblast population (Figure 2.2C). These data show that *Hoxa11eGFP* is strongly

Figure 2.2

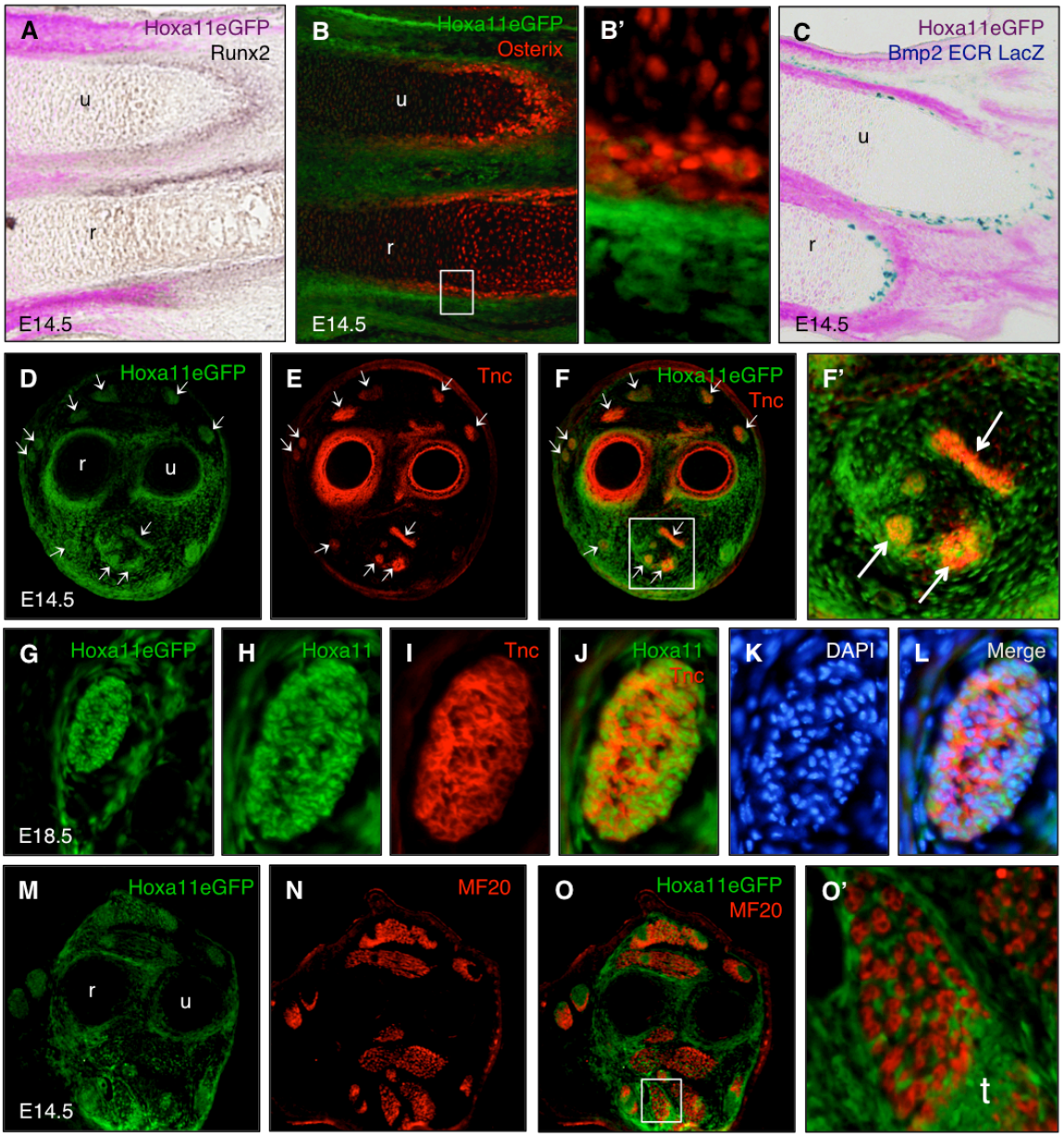
A
Hoxa11eGFP
Runx2
u
r
E14.5
B
Hoxa11eGFP
Osterix
u
r
E14.5
B'
C
Hoxa11eGFP
Bmp2 ECR LacZ
u
r
E14.5
D
Hoxa11eGFP
r
u
E14.5
E
Tnc
F
Hoxa11eGFP
Tnc
F'
G
Hoxa11eGFP
E18.5
H
Hoxa11
I
Tnc
J
Hoxa11
Tnc
K
DAPI
L
Merge
M
Hoxa11eGFP
r
u
E14.5
N
MF20
O
Hoxa11eGFP
MF20
O'
t

Figure 2.2. *Hoxa11eGFP* is expressed in the outer perichondrium, tendons, and muscle connective tissue but excluded from chondrocytes, osteoblasts, muscle, and endothelial cells. Longitudinal sections through E14.5 forelimbs of *Hoxa11eGFP* heterozygous embryos co-labeled for osteoblast markers by *in situ* hybridization for Runx2 (brown, A), antibody staining for Osterix (red, B, B'), or LacZ staining for the Bmp2 ECR reporter (blue, C) shows that *Hoxa11eGFP* is not expressed in osteoblasts but in the adjacent cells of the outer perichondrium. (GFP fluorescence was converted in images A and C to allow color visualization.) Transverse sections along the proximodistal axis of the limb in the zeugopod of *Hoxa11eGFP* heterozygous embryos (D-O'). Costaining with an antibody to the tendon marker Tnc shows that *Hox11* is expressed in all zeugopod tendons (D-F'). Select tendons are marked by arrows. *Hoxa11eGFP* expression is observed in all cells of the tendon and surrounding cells of the tendon sheath through E18.5 (G-L). Antibody staining for the muscle marker MF20 demonstrates that *Hoxa11eGFP* is not expressed in muscle cells but in the cells closely associated with the muscle masses (M-O'). (t indicates tendon.)

expressed in a population of stromal cells immediately adjacent to the osteoblast layer in the outer periosteum.

To better analyze the expression of *Hoxa11eGFP* in the soft-tissue components of the musculoskeletal system, we examined transverse sections through the zeugopod. The extracellular matrix protein, TenascinC (Tnc), marks anatomically distinct tendons and tendon primordia of the limb (Chiquet and Fambrough, 1984; Kardon, 1998). *Hoxa11eGFP* is coexpressed with Tnc in all tendons of the zeugopod (Figure 2.2D-F'). Using DAPI, a nuclear stain, in conjunction with *Hoxa11eGFP* and Tnc, we demonstrate that all of the cells within the Tnc-positive tendon express *Hoxa11eGFP* (Figure 2.2D-F',G-L).

Comparison of *Hoxa11eGFP* expression in the muscle cell population using antibodies against myosin to stain differentiated muscle cells reveals that *Hoxa11* is not expressed within the differentiated muscle cells but within the lateral plate-derived limb stromal cells closely associated with the myotubes (Figure 2.2M-O'). *Hoxa11eGFP* positive cells are distributed throughout and surround each of the muscle masses of the zeugopod.

In addition to being excluded from differentiated muscle cells (Figure 2.3A-C), co-staining with platelet endothelial cell adhesion molecule (PECAM) shows *Hoxa11eGFP* is non-overlapping with the differentiated endothelial compartment of the limb as well (Figure 2.3D-F). Co-staining with the muscle connective tissue marker Tcf4 demonstrates that *Hoxa11eGFP* is expressed in the mesodermal fibroblasts dispersed throughout the muscle masses (Figure 2.3G-I, arrows). The close association of *Hoxa11eGFP* expressing cells with myotubes is apparent as early as E12.5 when the

Figure 2.3

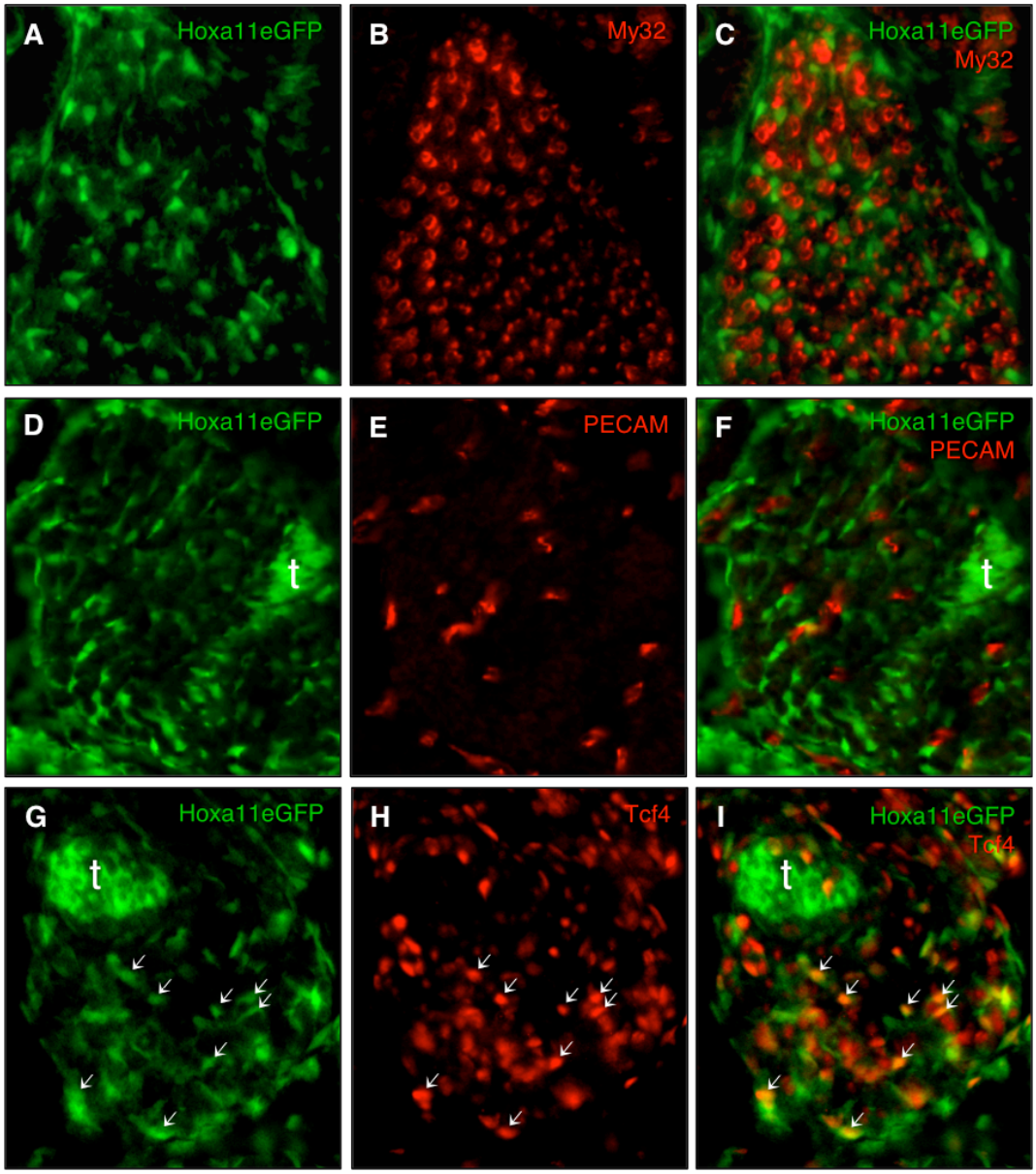

Figure 2.3. *Hoxa11eGFP* is expressed in muscle connective tissue but not endothelial cells or muscle cells. Transverse sections through forelimb zeugopod of *Hoxa11eGFP* heterozygous embryos at E14.5 (A-I). Antibody staining with the muscle marker My32 shows that *Hoxa11eGFP* is not expressed in muscle cells (A-C). *Hoxa11eGFP* is also excluded from the endothelial compartment marked with an antibody for PECAM (D-F). *Hoxa11eGFP* displays significant co-expression with antibody staining to the muscle connective tissue marker Tcf4 (G-I). Select *Hoxa11eGFP,* Tcf4 double positive cells are marked by arrows. (t indicates tendon.)

process of muscle splitting is initiated in the limb (Figure S2.1). Thus, *Hox11* is specifically expressed in the connective tissue population of the muscle throughout patterning but not in the muscle cells or the associated endothelial compartment.

Loss of *Hox11* function leads to defects in muscle patterning of the forelimb zeugopod

The expression of *Hox11* in muscle connective tissue during limb development led us to examine whether there is a role for *Hox11* in muscle patterning. Section analysis through control and *Hoxa11/d11* double mutant forelimbs stained with an antibody for differentiated muscle (My32) show that the stylopod muscle pattern of these animals are indistinguishable from controls (Figure 2.4A,C). In contrast, the zeugopod muscle pattern in *Hox11* double mutants is severely perturbed compared to controls (Figure 2.4B,D). Three-dimensional reconstructions of serial sections of My32-stained *Hox11* double mutant forelimbs at E14.5 allows visualization of the extent of muscle mispatterning in the zeugopod and putative identification of the remaining muscle masses based on their position within the limb as well as their origin and insertion sites. Several dorsal muscle groups in the mutants cannot be distinguished but appear as undivided muscle masses. These include the extensors carpi radialis brevis and longus and the extensors digitorum communis, lateralis, and carpi ulnaris (Figure 2.4D,G, #10-11, #12-14). Distal muscle groups of the dorsal zeugopod, such as the extensor policis and indicis proprius are absent in *Hox11* mutants (Figure 2.4E,G #15, #25). Additionally, many ventral muscle groups including the flexor digitorum superficialis 2, flexor digitorum profundus, and pronator quadratus are missing in *Hox11* double mutant forelimbs (Figure

Figure 2.4

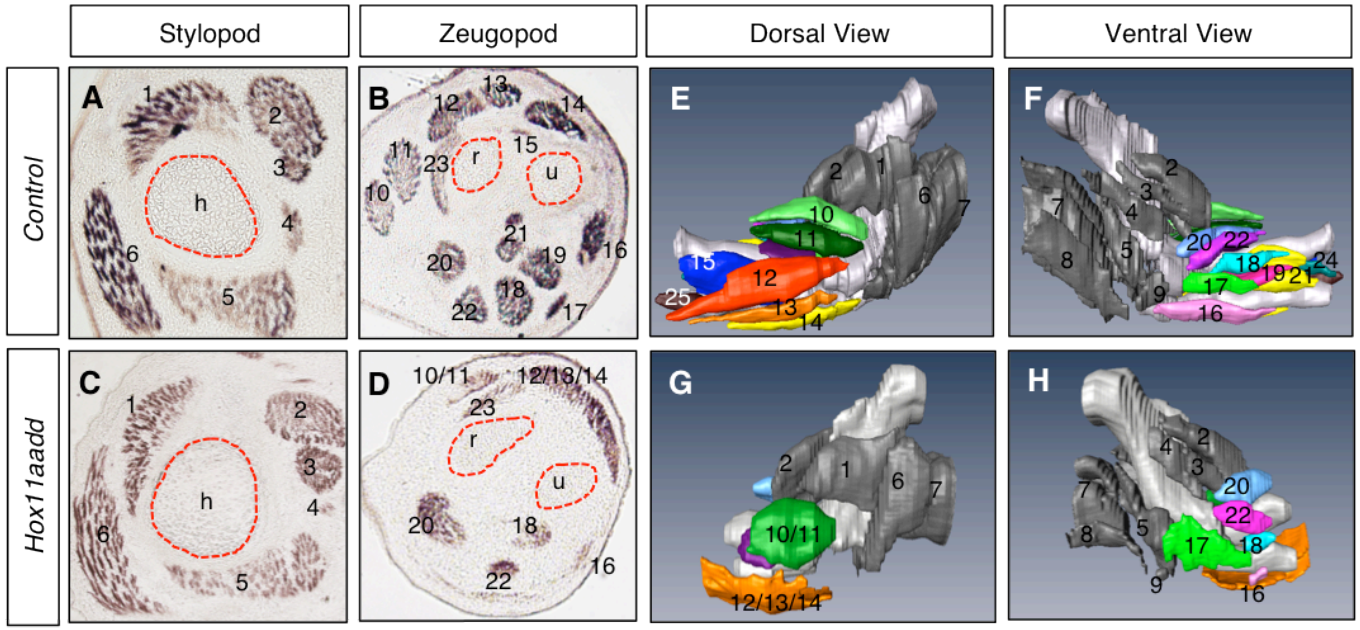

	Stylopod Muscles/Tendons
1	Brachialis
2	Biceps brachii long
3	Biceps brachii short
4	Corabrachialis
5	Triceps brachii medial
6	Triceps brachii lateral
7	Triceps brachii long
8	Dorsoepitraclearis brachii
9	Aconeus

	Zeugopod Muscles/Tendons
10	Extensor carpi radialis brevis
11	Extensor carpi radialis longus
12	Extensor digitorum communis
13	Extensor digitorum lateralis
14	Extensor carpi ulnaris
15	Extensor policis
16	Flexor carpi ulnaris
17	Palmaris longus
18	Flexor digitorum superficialis 1

19	Flexor digitorum superficialis 2
20	Pronator teres
21	Flexor digitorum profundus humeral, radial and ulnar head
22	Flexor carpi radialis
23	Supinator
24	Pronator Quadratus
25	Extensor indicis proprius

Figure 2.4. Forelimb zeugopod muscles are disrupted in *Hoxa11/d11* double mutants while stylopod muscles are unaffected. Transverse section through the stylopod of E14.5 control (A) and *Hox11* double mutant forelimbs (C) stained for differentiated muscle (∝My32) shows no difference in muscle pattern in this region in the absence of *Hox11*. The zeugopod of *Hox11* mutant (D) displays severe patterning defects compared to control (B). 3D reconstruction of serial sections stained with ∝My32 using Amira software (E-G). Numbers denote specific muscles listed in table below image. Many dorsal muscle groups are merged (10/11, 12/13/14) or absent (15) and several ventral muscle groups are absent (17, 19, 21).

2.4D,H #19, #20, #24). Reconstructions of sections through control and *Hox11* double mutant forelimb musculature demonstrate that the remaining muscle groups in mutants are highly dysmorphic compared to controls (Figure 2.4E-H).

Loss of *Hox11* function leads to disrupted tendon structure and pattern

Hoxa11/d11 mutant tendon progenitors arise normally and their initial pattern, as detected by *in situ* hybridization for *Scleraxis* (*Scx*), is indistinguishable from controls at E12.5 (Figure 2.5A,F). However, by E14.5, severe defects in the tendon structure and pattern are apparent in *Hox11* mutants compared to controls (Figure 2.5B-E,G-J). Staining for Tnc, a component of the tendon extracellular matrix, shows that the pattern of tendons in *Hoxa11/d11* mutants at this stage corresponds to the altered muscle pattern in these animals. In instances where muscles are absent, no associated tendon is observed by E14.5 (Figure 2.5G-I). In the dorsal zeugopod of *Hoxa11/d11* double mutants, the three tendons associated with the extensors digitorum communis, lateralis, and carpi ulnaris, which are an undivided single muscle mass in mutant embryos, are formed as normal separated tendons in the autopod, but then fuse to make a myotendinous junction with the single muscle mass in the zeugopod (Figure 2.5G-I, asterisks). In addition to disrupted patterning, the tendons formed in *Hox11* mutants lack proper organization and do not fasciculate as observed for controls (Figure 2.5E,J).

Remaining *Hox11* mutant tendons are smaller than controls at E18.5 and histological examination shows that it is difficult to discern the tendon sheath in *Hox11* mutant tendons (Figure 2.6A,A',B,B'). The tendon sheath is an elastic sleeve of connective tissue that surrounds the tendon and functions to provide lubrication to

Figure 2.5

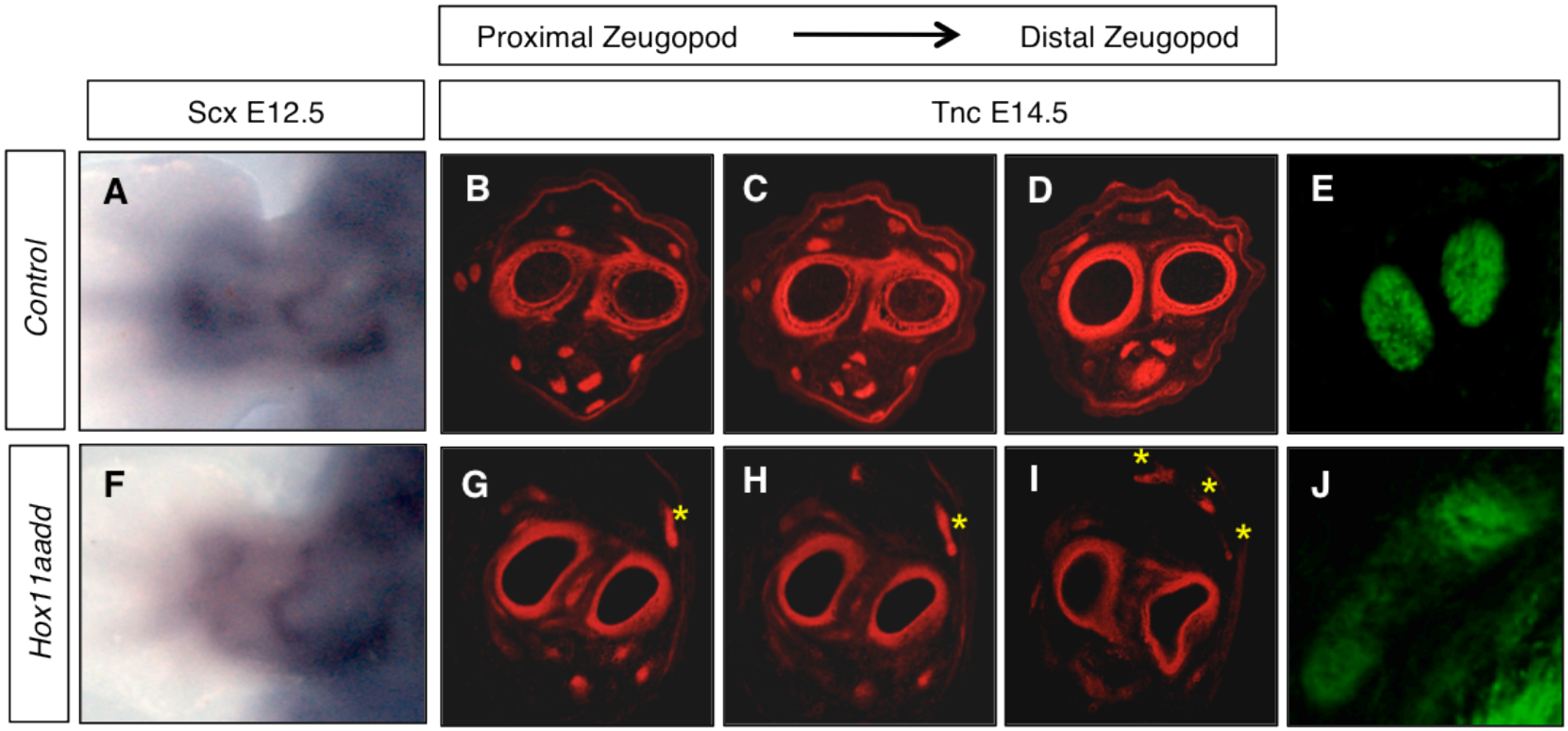
Proximal Zeugopod
Distal Zeugopod
Scx E12.5
Tnc E14.5
Control
Hox11aadd
A
B
C
D
E
F
G
H
I
J

Figure 2.5. Tendon patterning is disrupted in the forelimb zeugopod of *Hox11* double mutants. Whole mount *in situ* hybridization for the tendon marker Scleraxis in control (A) and *Hoxa11*/*d11* double mutant (F) forelimbs at E12.5 shows that tendon progenitors are normally specified in *Hox11* mutants. Transverse sections through the zeugopod of control (B-D) and *Hoxa11/d11* (G-I) forelimbs at E14.5 from proximal (left) to distal (right) stained with an antibody for Tnc to detect tendons. The pattern of tendons in *Hox11* mutants at this stage correlates with the altered muscle pattern in these animals. High magnification of Tnc stained tendon in control (E) and *Hox11* double mutant (J) shows disorganization of remaining tendons

minimize friction between the tendon and surrounding tissues. Tubulin polymerization-promoting protein family member 3 (Tppp3) has been identified as a molecular marker of the cells of the tendon sheath (Staverosky et al., 2009). Hyaluronic acid (HA) and Lubricin are main components of the synovial fluid that surround the tendon and are important for normal tendon function (Kohrs et al., 2011). Marker analysis with Tppp3 shows that tendon sheath cells are present in the proper location surrounding the tendons in *Hox11* double mutants (Figure 2.6C,D). However, HA and Lubricin are dramatically reduced or absent from zeugopod tendon synovium with loss of *Hox11* function (Figure 2.6E-H).

Tendons are composed of closely packed parallel collagen fiber bundles that are essential for providing the tensile strength required for transmitting loads (Wang et al., 2012). In the zeugopod tendons of *Hox11* double mutant embryos at E18.5, Sirius Red staining for collagen is reduced compared to controls, consistent with either a reduction in collagen or an alteration in collagen organization (Figure 2.7A,B (Puchtler et al., 1973; Sweat et al., 1964)). To examine this further, we performed transmission electron microscopy (TEM) on transverse sections through zeugopod tendons of control and *Hox11* mutants. While *Hox11* mutant tendons are notably smaller, as observed histologically, no gross differences are observed in the amount of collagen (Figure 2.7B, E and Figure S2.2). However, the organization of the collagen fibers is markedly disrupted. In control tendons, collagen fibers run uniformly perpendicular to the plane of section resulting in round cross sections of even diameter (Figure 2.7B). The collagen fibers in *Hox11* mutant tendons are disorganized and run in multiple directions, both

Figure 2.6

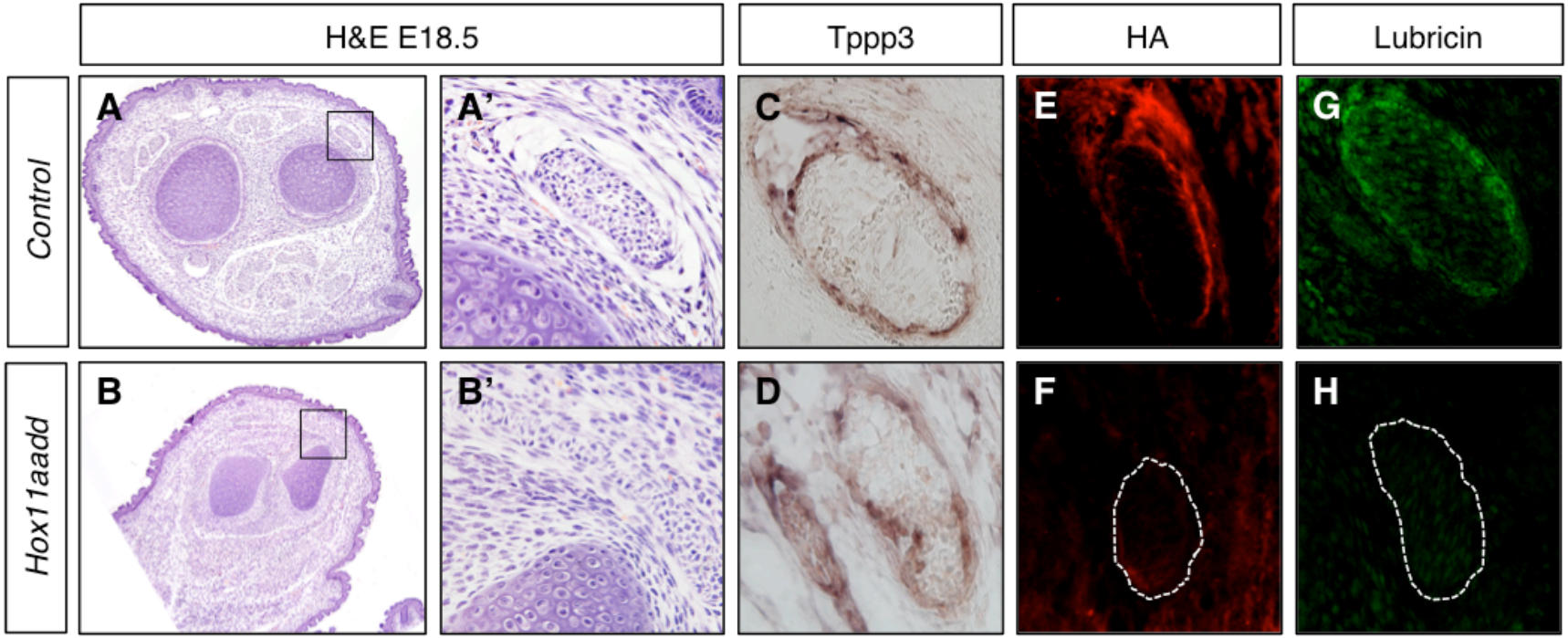

Figure 2.6. In the absence of *Hox11* function, tendon structure is abnormal and tendon sheath extracellular matrix is not present. Transverse sections through the zeugopod of control (A, C, E, G) and Hoxa11/d11 mutant (B, D, F, H) forelimbs at E18.5. Hematoxylin and Eosin (H&E) staining (A, A', B, B') shows abnormal tendon histology in *Hox11* mutants. *In situ* hybridization for the tendon sheath marker Tppp3 (C, D) demonstrates presence of tendon sheath cells. Staining for components of the tendon extracellular matrix hyaluronic acid (HA) (red E, F) and ∝-lubricin (green G, H) is dramatically reduced surrounding the tendon of *Hox11* mutants.

Figure 2.7

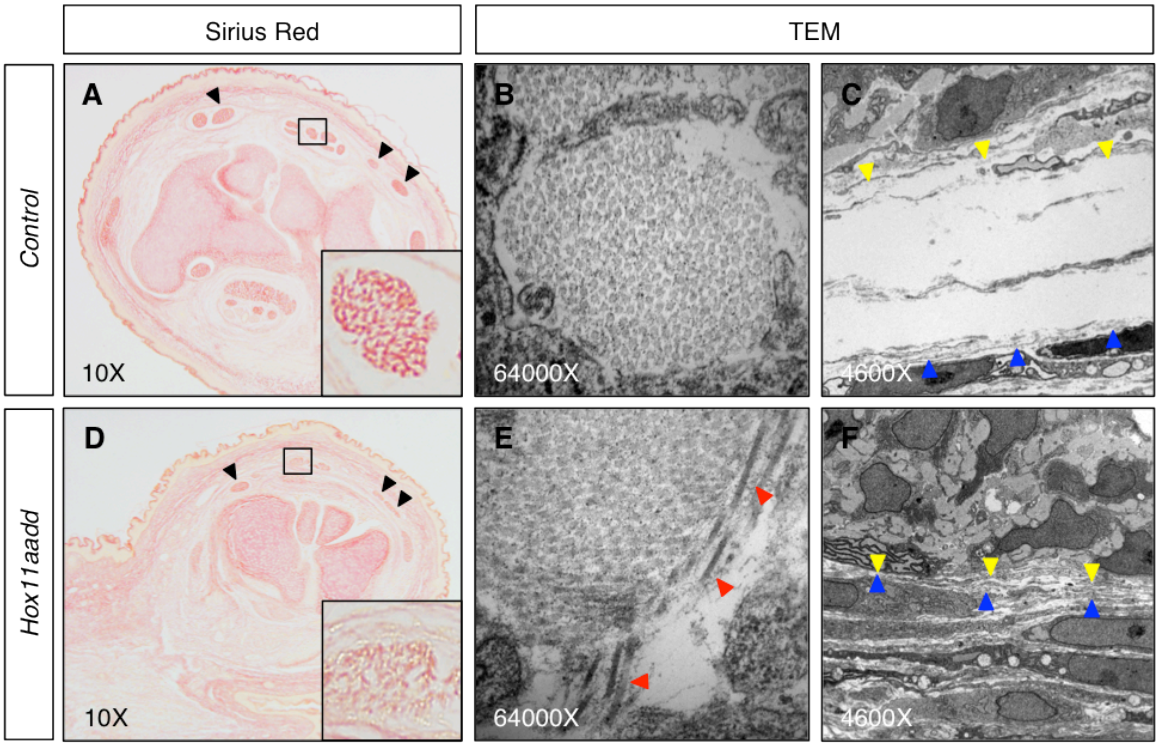

Figure 2.7. Tendons of *Hox11* mutants have disorganized collagen fibers. Sirius red staining for collagen is reduced in *Hox11* double mutant (D) zeugopod tendons at E18.5 compared to control (A). Black arrowheads indicate three dorsal tendons. Transmission electron microscopy (TEM) images of collagen fibers in control (B) and *Hox11* mutant (E) forelimb zeugopod tendon show disorganization of collagen in *Hox11* mutant. Red arrowheads point to collagen fibers running parallel to the plane of section, opposite to the normal orientation. Synovial fluid-filled space surrounding the tendon in control sections (C) is not observed around tendons in *Hox11* mutants (F). Yellow arrowheads indicate boundary of tendon fibroblasts. Blue arrowheads indicate boundary of tendon sheath cells.

perpendicular and parallel to the plane of section (Figure 2.7E, red arrowheads mark misaligned fibers). Additionally, the synovial space surrounding the tendon can be clearly observed in controls (Figure 2.7C) but this region is absent in *Hox11* mutant tendons (Figure 2.7F). In mutants, the collagen and tendon fibroblasts that make up the body of the tendon are observed directly adjacent to tendon sheath cells with no extracellular matrix deposition between these layers.

Muscle and tendon patterning defects in *Hox11* mutants are independent of skeletal development

In addition to the previously appreciated role for *Hox* genes in patterning the skeleton, we show here that muscle and tendon formation are also severely disrupted in the forelimb zeugopod of *Hoxa11/d11* mutant embryos. Further, we show that *Hoxa11eGFP* expression can be observed in the tendon and muscle connective tissue from the earliest stages in addition to the perichondrium of the developing zeugopod skeleton. However, it is not possible to distinguish whether the defects in muscle and tendon are primary or secondary to the defects in skeletal patterning. In *Hoxa11/d11* mutant embryos, the disruption of muscle, tendon and skeletal patterning becomes apparent at approximately the same developmental stages. To separate potential effects of the skeletal malformations from the function of *Hox11* genes in soft tissue patterning, we analyzed the muscle and tendon pattern in *Hox11* compound mutants in which three of four *Hox11* alleles are mutant. Due to the high degree of functional redundancy among members of a paralogous group, when a single allele of *Hoxa11* or *Hoxd11* remains functional, the skeletal elements of the zeugopod develop relatively normally

through newborn stages (Figure 2.8A) (Boulet and Capecchi, 2004; Davis et al., 1995). Despite the normal skeletal phenotype in *Hox11* compound mutants, significant disruption in muscle and tendon patterning are observed. Section analyses at E14.5 shows abnormal splitting of dorsal muscle groups in compound mutants. In Hoxa11$^{+/-}$;d11$^{-/-}$ or Hoxa11$^{-/-}$;d11$^{+/-}$ animals, the extensor digitorum comunis and lateralis fail to separate but unlike double mutants, the extensor carpi ulnaris is patterned normally (Figure 2.8B-D, red arrowheads). Some compound mutant embryos also lack a separation between the extensor carpi radialis brevis and longus muscles (Figure 2.8C, blue arrowhead). Sections at E14.5 reveal more severe disruptions in the patterning of the ventral zeugopod muscle groups in *Hox11* compound mutants as well, with all mutant ventral muscle groups appearing less organized (Figure 2.8B-D, brackets). Additionally, tendon patterning is severely disrupted in *Hox11* compound mutants. Immunohistochemistry for Tnc at E14.5 shows that *Hox11* compound mutant tendons are smaller than controls, and multiple tendons are missing from the ventral region by E14.5 (Figure 2.8E-G). These experiments demonstrate that the defects in tendon and muscle patterning are independent of skeletal malformation.

Figure 2.8

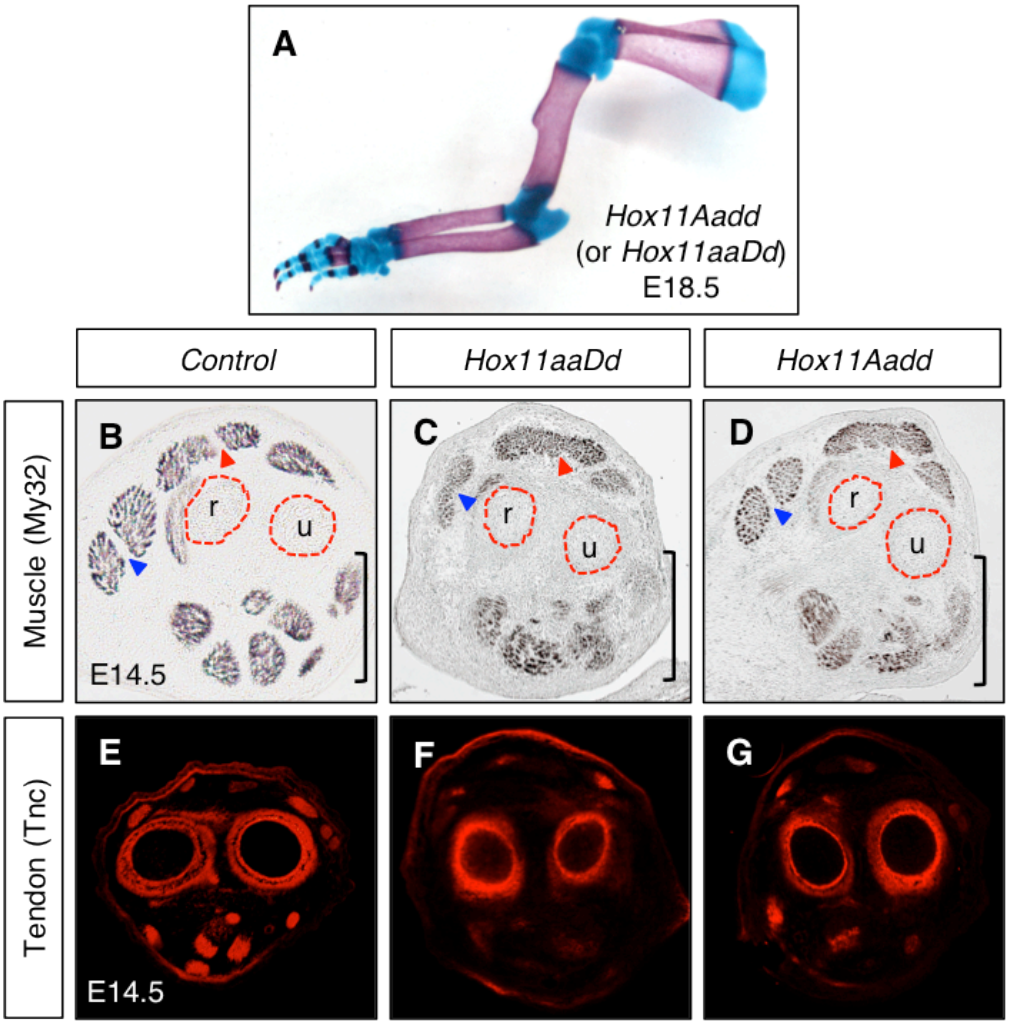

Figure 2.8. *Hox11* compound mutants display normal skeletal patterning, however muscle and tendon patterning is disrupted. Alcian blue and alizarin red stained skeletal preparation of an E18.5 *Hox11* compound mutant (*Hoxa11*$^{+/-}$; *Hoxd11*$^{-/-}$) (A) shows that the zeugopod skeletal elements are patterned normally when only one of the four *Hox11* alleles is wild-type. Antibody staining for differentiated muscle (∝My32) in transverse sections through the zeugopod of control (B) and *Hox11* compound mutants (C, D). No separation is observed between the extensor digitorum communis and lateralis in compound mutants (red arrowhead) or between the extensor carpi radialis brevis and longus in Hoxa11$^{-/-}$;d11$^{-/+}$ (blue arrowhead). Ventral muscle groups are severely disorganized in compound mutants (C, D, bracket). Transverse sections through the distal zeugopod of control (E) and *Hox11* compound mutant (F, G) forelimbs at E14.5 stained with an antibody for Tnc to detect tendons shows disrupted tendon formation in *Hox11* compound mutants compared to control.

DISCUSSION

Much of our current understanding of the role of *Hox* genes in patterning has arisen from analyses of *Hox* loss-of-function skeletal phenotypes. Despite the well-known skeletal phenotypes of loss-of-function *Hox* mutants, herein we demonstrate that *Hox11* gene expression is largely excluded from the skeletal elements. Our results show that *Hoxa11eGFP* is expressed broadly throughout the limb bud at early stages and becomes restricted to the outer perichondrium, tendons, and muscle connective tissue fibroblasts of the zeugopod region as the skeletal anlage condense. Cells of the perichondrium secrete a variety of factors that profoundly influence chondrogenic differentiation (Karsenty, 2008; Kronenberg, 2007). These data suggest that *Hox* genes may exert their influence on skeletal development by regulating the expression of paracrine factors within the perichondrium and thereby directing the growth of the underlying cartilage.

With the loss of *Hoxa11* and *Hoxd11* function, tendon precursor cells appear to be specified normally much like zeugopod cartilage templates are specified appropriately, however, tendon patterning in the zeugopod region is severely disrupted. Tendons are specialized connective tissue cells that function to link muscle to bone and modulate forces during movement. Tendon primordia arise from within the limb mesenchyme in dorsal and ventral areas of the limb and subsequently align between the muscle masses and skeletal elements (Schweitzer et al., 2001). Later, tendon morphogenesis requires the presence of muscles, as tendon progenitors are progressively lost in the absence of muscle invasion (Bonnin et al., 2005; Edom-Vovard et al., 2002; Kardon, 1998; Kieny and Chevallier, 1979). Tendon ablation experiments suggest that tendons contribute to

muscle patterning by restricting muscle domains during development (Kardon, 1998). In *Hox11* mutants, tendon progenitors are observed, but they do not differentiate normally, they display poor fasciculation and some tendons in the zeugopod region fail to form. The high expression levels of *Hoxa11eGFP* in all cells of the tendons suggest a direct role for *Hox* genes in tendon morphogenesis.

Our results also demonstrate a severe disruption in zeugopod muscle patterning with loss of *Hox11* function while other limb regions are unaffected. In contrast to the other components of the limb musculoskeletal system such as the bone, tendons, and muscle connective tissue that arise from cells within the lateral plate mesoderm, muscle cells migrate from the axial somites into the limb bud where they proliferate, aggregate and differentiate to form dorsal and ventral muscle masses. These masses subsequently segregate into individual, anatomically distinct muscle masses to achieve the final muscle pattern (Chevallier et al., 1977; Christ et al., 1977b; Ordahl and Le Douarin, 1992; Wachtler et al., 1981). Embryologic manipulation experiments have shown that muscle cells do not posses intrinsic regulatory information for establishing pattern; rather, this information is transmitted through cells in the lateral plate mesoderm. In experiments where somites from axial levels outside the normal limb region were transplanted to replace limb level somites, the muscle cells migrated into the limb and were able to give rise to normal limb muscle (Chevallier et al., 1977; Christ et al., 1977b). In addition, classic chick-quail graft experiments and single-cell lineage analysis of muscle precursor cells revealed that individual myogenic cells are not predetermined to form any particular anatomical muscle (Chevallier et al., 1977; Christ et al., 1977a; Christ et al., 1977b; Kardon et al., 2002). These studies indicate that cells within the limb mesenchyme

provide the cues required for muscle pattern. Experiments with muscle-less limbs have shown that muscle connective tissue organizes into distinct morphological groups in the absence of muscle invasion suggesting that muscle connective tissue regulates the patterning of migrating myoblasts (Chevallier and Kieny, 1982; Grim and Wachtler, 1991). The factors responsible for patterning the muscle are not well understood. The data we report here supports a role for *Hox* genes in regional muscle patterning through their expression in the connective tissue.

The zeugopod skeleton of *Hox11* double mutants is dramatically shortened raising the question of whether muscle and tendon defects observed in these animals might, in fact, be secondary to perturbations in skeletal morphology. To address this, we analyzed *Hox11* compound mutant limbs in which a single *Hox11* allele remains functional, allowing the skeleton to develop normally through embryonic stages. Muscle and tendon patterning is also disrupted in these animals, demonstrating that these defects are not an indirect results of skeletal perturbation but represent an independent patterning role for *Hox* genes in the soft-tissue components of the musculoskeletal system.

While *Hox* expression in early limb buds prior to the differentiation of mesoderm into specific tissue cell types is broad, this expression quickly becomes localized to the limb region where its patterning function is observed. Expression is largely confined at these stages to the connective tissues. This expression persists throughout development in the connective tissue cells. Previous studies of *Hox* expression and function within the limb have primarily focused on the early, broad expression of *Hox* genes in the limb mesenchyme and relied on whole mount analyses of limb buds rather than more detailed

examination of tissue-specific expression patterns. Our results suggest a possible continued role for *Hox* genes throughout limb development.

During development, muscle, tendon and bone must be tightly coordinated to produce a functional system. However, the formation of each of these tissues is often studied separately. Thus, significant knowledge on the mechanisms of differentiation of each of these individual tissues has been attained; however, much less is known regarding how these tissues are integrated. Our results demonstrate that *Hox* genes are critical not only for patterning the skeleton but also for patterning muscle and tendon to produce a regionally integrated, functional musculoskeletal system. This study illustrates the essential role of *Hox* genes in patterning the vertebrate body plan and shifts the paradigm of *Hox* function in musculoskeletal development from one where these genes are critical factors for skeletal morphogenesis to one that recognizes their role in the patterning and integration of all musculoskeletal tissues.

MATERIALS AND METHODS

Animals

Male and female mice heterozygous for both the *Hoxa11* and *Hoxd11* null alleles were mated to generate compound mutant and double mutant embryos as previously described (Boulet and Capecchi, 2004). Embryos heterozygous for the *Hoxa11eGFP* allele were generated by traditional breeding strategies as previously described (Nelson et al., 2008). All animal experiments performed in this report were reviewed and approved by the University of Michigan's Committee on Use and Care of Animals, Protocol #08787.

In situ hybridization and immunohistochemistry

Whole mount *in situ* hybridization (ISH) was performed as previously described (Huppert et al., 2005; Wellik et al., 2002). For section ISH, embryos were collected in PBS and fixed overnight in 4% paraformaldehyde in PBS at 4°C. Embryos were then rinsed in PBS and immersed in 30% sucrose at 4°C overnight prior to embedding into OCT media. Section ISH was performed as previously described (Di Giacomo et al., 2006; Mendelsohn et al., 1999). Prior to ISH on sections of *Hoxa11eGFP* tissue, slides were rinsed in PBS and fluorescent images were taken on an Olympus BX-51 upright light microscope with an Olympus DP70 camera. Runx2, Scx and Tppp3 in situ probes were previously described (Murchison et al., 2007; Staverosky et al., 2009).

For immunohistochemistry (IHC) on sections, embryos were processed and sectioned as described above for section ISH. For whole mount IHC, embryos were collected in PBS and the skin was removed from the limbs by careful dissection prior to fixation overnight in 4% paraformaldehyde in PBS at 4°C prior to transfer through a graded series of methanol. Immunohistochemical staining was performed using antibodies for Sox9 (1:500, Millipore, AB5535), TenascinC (1:400, Sigma, T3413), GFP (1:500, Invitrogen, A-11122), MF20 (1:50, Developmental Studies Hybridoma Bank), My32 (alkaline phosphatase conjugated, 1:800, Sigma, A4335, unconjugated, 1:200, Sigma, M4276), and Lubricin (1:200, Thermo Scientific, PA3-118). Antibody staining for Tcf4 (1:100, Cell Signalling, 2569 C48H11) was performed on flash frozen tissue without detergent. To visualize hyaluronic acid, a biotinylated hyaluronic acid binding

protein (HABP, Calbiochem) was used as previously described (Calve et al., 2010). β-Galactosidase staining was performed as described (Mortlock, 2003).

Three-dimensional reconstruction of serial sections

Embryos were collected at E14.5 and processed for IHC as described above. 20 μm serial sections were stained for My32. Serial section images were loaded into the program Amira 4.1 (Visage Imaging Inc., Andover, MA) and automatically aligned using the least-squares function of the Amira AlignSlices tool. Automatically aligned stacks were manually corrected if necessary. My32 stained muscle masses were selected using the LabelField tool and a 3D surface was generated from the selected fields.

ACKNOWLEDGEMENTS

This manuscript was written by Ilea T. Swinehart, Aleesa J. Schlientz, Christopher A. Quintanilla, Douglas P. Mortlock, and Deneen M. Wellik. It was submitted in March 2013 to Development.

Our thanks to investigators who provided reagents for experiments reported here. The HABP and Lubricin antibody were provided by Dr. Christoper L. Mendias. The Tppp3 and Scx *in situ* probes were provided by Dr. Ronen Schweitzer. The Runx2 *in situ* probe was provided by Dr. Renny T. Franceschi. We thank Dr. Chris Mendias, Dr. Sarah Calve, Dr. Steven M. Hrycaj and Danielle R. Rux for their comments and suggestions.

This study was supported in part by NIH AR061402 (D.W.) and AR057018 (D.W.), by the NIH Cellular and Molecular Biology Training Grant T32-GM007315 (I.S.) and by the Michigan NIH PREP Program Training Grant F033036 (C.Q.).

Figure S2.1

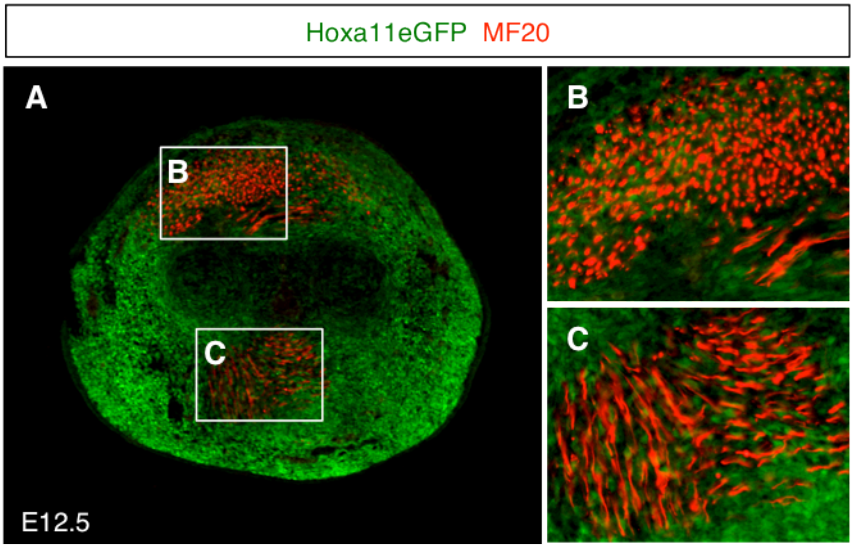

Figure S2.1 *Hoxa11eGFP* is expressed in cells closely associated with muscle from the earliest stages of muscle patterning. Section through E12.5 *Hoxa11eGFP* (green) forelimb zeugopod stained with an antibody for muscle myosin (MF20, red).

Figure S2.2

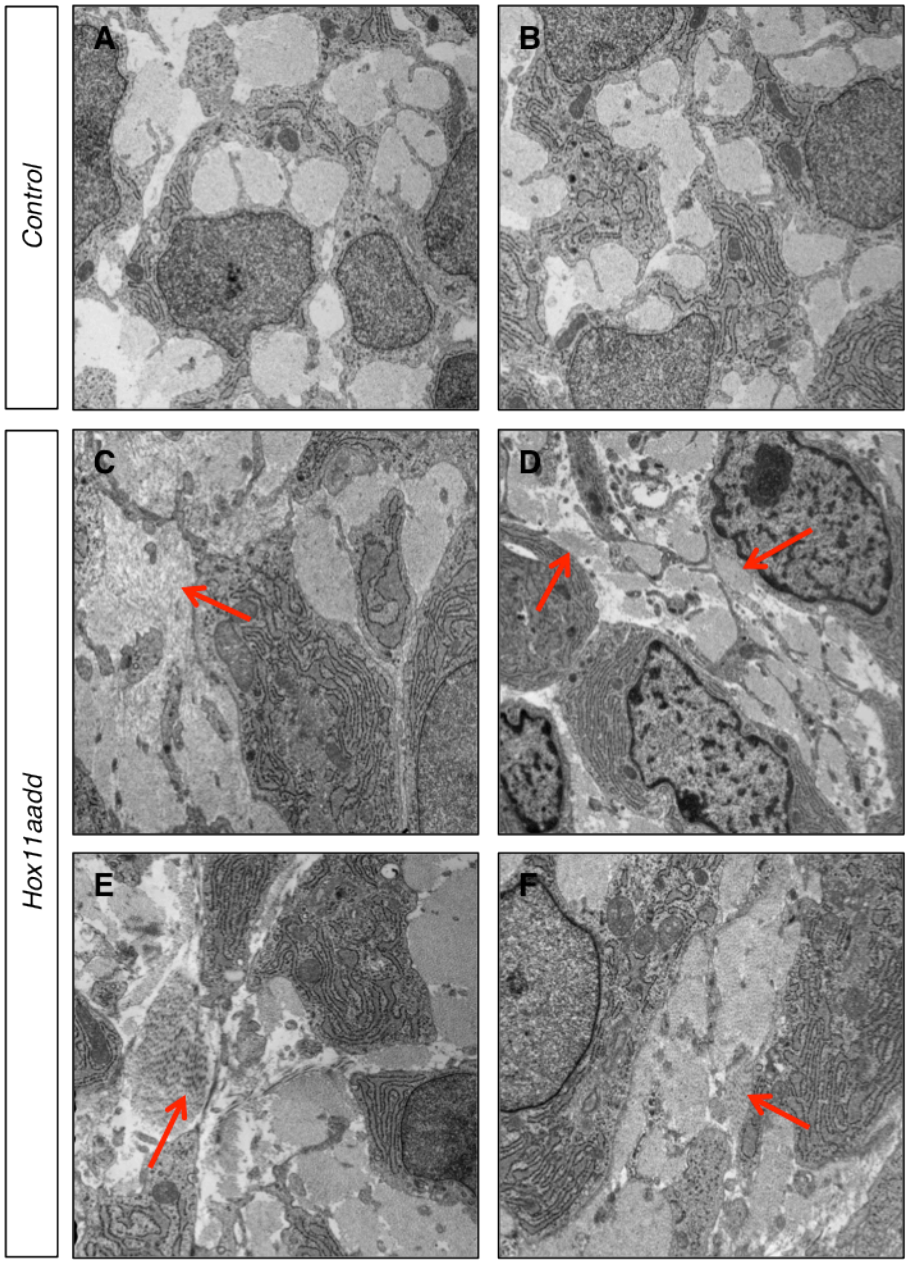

Figure S2.2 Collagen fibrils are disorganized in *Hox11* mutant tendons. TEM of transverse sections through forelimb zeugopod tendons of control (A, B) and *Hox11* double mutant (C-F). Red arrows indicate areas in mutant where collagen fibrils run abnormally parallel to the plane of section.

CHAPTER III

HOX11 GENES PLAY A PIVOTAL ROLE IN FRACTURE INJURY RESPONSE AND SKELETAL REPAIR

SUMMARY

Hox genes are critical regulators of skeletal patterning during embryogenesis. During development, these transcription factors are expressed in domains along the AP axis of the body and PD axis of the limb. Recent evidence suggests that *Hox* expression is maintained throughout adult life and at least some aspects of the regionally restricted pattern observed during embryogenesis are conserved. A careful analysis of *Hoxa11* expression at postnatal and adult stages demonstrates that *Hox11* remains regionally expressed in skeletal tissues throughout adult life and is up-regulated in the fracture callus during repair. To examine the function of *Hox11* during fracture repair, we assessed the healing of *Hox11* compound mutants in which three of the four *Hox11* alleles are null. Fracture healing is impaired in *Hox11* compound mutants. Ulnar fractures in these animals show reduced callus cartilage formation, demonstrating that *Hox11* genes are important for the early phase of bone repair.

INTRODUCTION

Hox genes are well known for patterning the vertebrate body plan. During development, *Hox* expression follows a co-linear pattern along the axial skeleton where these genes are responsible for providing regional patterning information (Mallo et al., 2010; McIntyre et al., 2007; Wellik, 2007; Wellik and Capecchi, 2003). The posterior *Hox* genes, paralogous groups 9-13, are expressed in domains along proximal-distal of the limb where they also perform regional patterning roles (Chapter I, Figure 1.3 (Boulet and Capecchi, 2004; Davis et al., 1995; Fromental-Ramain et al., 1996b; Wellik and Capecchi, 2003; Zakany and Duboule, 2007)). In the limb, paralogous loss of function results in loss of patterning within specific limb regions while other regions of the limb remain largely unaffected. A striking example of this is paralogous loss-of-function of *Hox11* genes in which the zeugopod skeletal elements (radius/ulna and tibia/fibula) are severely truncated (Boulet and Capecchi, 2004; Davis et al., 1995; Wellik and Capecchi, 2003). While much of the research on *Hox* genes patterning in mammals has focused solely on the skeleton, recent work shows that *Hox11* genes function within the limb connective tissue to provide regional patterning information to muscle and tendon as well as the developing skeleton (Chapter II (Swinehart et al., submitted)).

Expression profiling studies have shown that regional *Hox* expression continues throughout the life of the organism, especially in tissues that undergo frequent renewal. Comparison of the gene expression programs of adult fibroblasts from numerous anatomic sites across the human body shows specific *Hox* expression patterns that are determinants that allow an indication of the position of the cell along the anterior-posterior, dorsal-ventral, and proximal-distal axes (Rinn et al., 2006). Differential *Hox*

expression has been reported in other adult tissues including smooth muscle and fat deposits as well (Chi et al., 2007; Gesta et al., 2006). Further, Ackema et al. showed that mesenchymal stem cells display region-specific *Hox* expression profiles (Ackema and Charité, 2008).

The adult skeleton is a dynamic tissue that undergoes continual remodeling throughout adult life. Skeletal tissues have the ability to repair in response to injury to reestablish the original tissue morphology and recover biomechanical function of the damaged tissue. However, the mechanisms by which these tissues recover the appropriate morphology during remodeling and repair are not well understood. Increasing evidence suggests that *Hox* genes may be important throughout adult life for healing and repair processes (Leucht et al., 2008; Rinn et al., 2008).

A remarkable amount of reorganization and remodeling occurs during fracture healing. How a large, disorganized mass of cartilage and bone is remodeled to return to the original size and shape of the unfractured skeleton is not well understood. Elucidating the regulatory molecules involved in this process could be critical for improving therapies related to skeletal repair and regenerative medicine. Fracture healing is a specialized repair process that recapitulates many of the aspects of embryological skeletal development (Ferguson et al., 1999; Vortkamp et al., 1998). Skeletal repair requires patterning cues from the local environment as is true during skeletal development; however, little is understood regarding the mechanisms for these processes (Campbell and Kaplan, 1992; Kaplan and Shore, 1996; Zimmermann et al., 2012).

The process of skeletal repair is defined by functional and morphological stages. There is an initial inflammatory cell influx, followed by mesenchymal cell proliferation

and vascularization, chondrogenic and osteogenic differentiation, endochondral and intramembranous bone formation, and finally remodeling. Possible roles for *Hox* genes in these processes have not previously been investigated.

To begin to address the question of whether Hox genes play a role in fracture repair, we utilized a *Hoxa11eGFP* knock-in/knock-out allele to examine *Hox11* expression in the limb at postnatal and adult stages and during the process of fracture repair. We report here that *Hox11* is expressed throughout adult life in the periosteum of zeugopod skeletal elements in a pattern very similar to what is observed developmentally. *Hox11* expression is also maintained regionally in the endosteum of the zeugopod. During fracture healing, *Hox11* expression in the surrounding periosteum is widely up-regulated throughout the fracture callus from the soft callus stage through callus remodeling stages. Surprisingly, strong *Hox11* expression is observed during the remodeling stage when a large proportion of the cell population consists of hematopoetic-derived osteoclasts. The continued postnatal expression of *Hox11* in skeletal tissues and up-regulation following injury suggests that *Hox* genes may provide patterning cues for skeletal remodeling and repair.

To address a possible function of *Hox11* genes during fracture repair, we compared fracture repair in *Hox11* compound mutants and wild-type controls. *Hox11* compound mutants used in these analyses are heterozygous for *Hoxa11* and homozygous null for *Hoxd11*. They therefore have only one functional *Hox11* allele in the forelimb (the third member of the *Hox11* paralogous group, *Hoxc11*, is not expressed in this region (Hostikka and Capecchi, 1998)). Using these mutants provides a genetic model of reduced *Hox* function that still permits relatively normal developmental patterning. We

observed a significant reduction in cartilage formation and delay in mineralization across the fracture gap in *Hox11* compound mutants. These data demonstrate that *Hox11* function is required for normal callus formation and healing after skeletal fracture.

RESULTS

Hoxa11eGFP is expressed in skeletal tissues throughout postnatal stages

Hox11 genes are expressed in the limb bud mesenchyme from early stages of limb development and are essential for patterning of the zeugopod skeletal elements (Boulet and Capecchi, 2004; Haack and Gruss, 1993; Hostikka and Capecchi, 1998; Hsieh-Li et al., 1995; Nelson et al., 2008; Small and Potter, 1993; Wellik and Capecchi, 2003). *Hox11* expression surrounds the distal radius/ulna and tibia/fibula throughout embryogenesis (Chapter II, Figure 2.1 (Swinehart et al., submitted)). During limb development, *Hox11* expression is localized to the connective tissue compartment of the limb including the muscle connective tissue, tendons and outer periosteum surrounding the zeugopod skeletal elements (Figure 2.2 and Figure 2.3). We examined the expression of *Hoxa11* in adult limbs using a previously described *Hoxa11eGFP* knock-in, knock-out allele that has been shown to closely recapitulate the dynamic expression patterns of *Hoxa11* (Nelson et al., 2008). We examined the expression of *Hoxa11eGFP* in the forelimb at four and twelve weeks of age. *Hoxa11eGFP* is expressed in the periosteum, the membrane lining the outer surface of the bone which contains progenitor cells that develop into osteoblasts and chondrocytes during repair (Figure 3.1, red arrowheads)

Figure 3.1

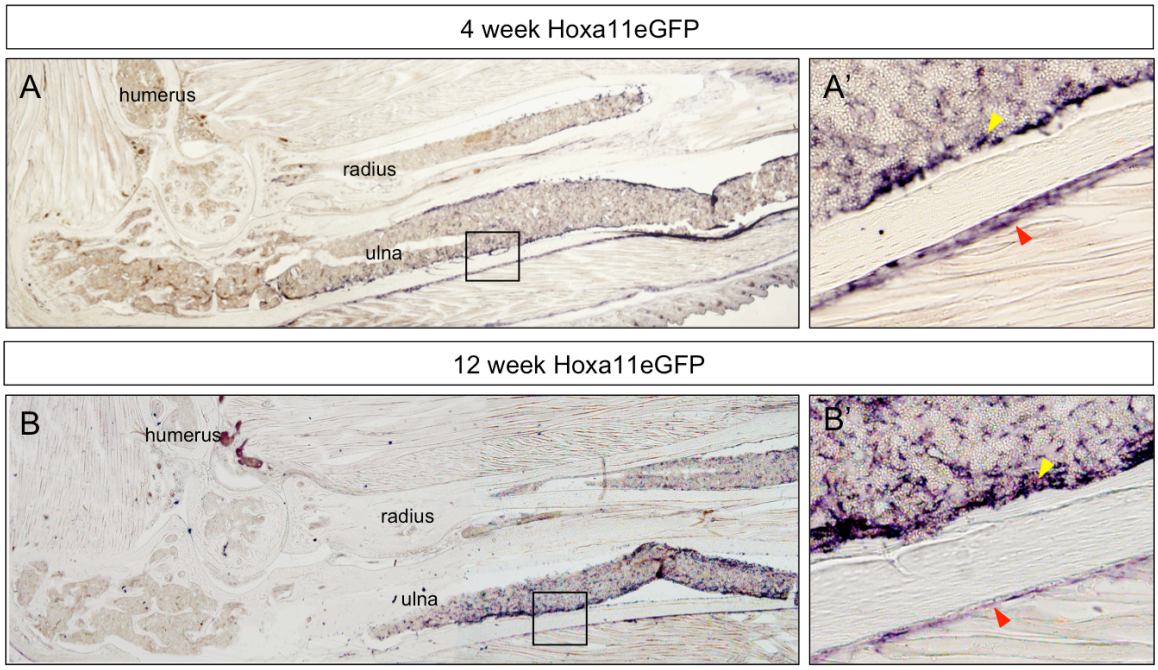

Figure 3.1. *Hoxa11eGFP* expression in postnatal and adult skeletal tissues. *Hoxa11eGFP* is expressed at postnatal and adult stages in the zeugopod periosteum (red arrowheads), endosteum (yellow arrowheads) and bone marrow. *Hoxa11* expression is detected by antibody staining for GFP in sections through the forelimb of *Hoxa11eGFP* heterozygous animals at 4 weeks (A, A') and 12 weeks (B, B') after birth.

(Malizos and Papatheodorou, 2005). *HoxalleGFP* expression is additionally observed along the endosteal surface of the radius and ulna (Figure 3.1, yellow arrowheads). *Hoxa11eGFP* is also expressed in cells throughout the bone marrow of the radius and ulna (Figure 3.1). The expression of *Hoxa11eGFP* is distally restricted to approximately half of the length of the radius and two-thirds of the ulna. Consistent with developmental *Hox11* expression patterns, no *Hoxa11eGFP* expression is observed in the bone marrow cells or periosteum of the humerus during adult stages (Figure 3.1).

Hoxa11eGFP **is up-regulated during fracture repair**

Hoxa11 expression has been reported in the tibial periosteum of adult mice as well as in cells within the injury site after fracture (Leucht et al., 2008). However, the details of the timing and cellular localization of *Hox* expression during skeletal repair have not been reported. We examined the expression of *Hoxa11* using the *Hoxa11eGFP* allele at 1.5 and 3 weeks post fracture (WPF) in both tibial and ulnar fracture models.

The 1.5 week time point represents the soft callus phase of fracture repair. At this stage, the callus is primarily composed of cartilage. The cells at the periphery of the cartilage are beginning their maturation to hypertrophy around this stage (Gerstenfeld et al., 2003; Ushiku et al., 2010). Mineralized tissue forms in triangular zones from the periosteal regions of the original bone and encroaches on the cartilage core. At 1.5 WPF in the tibia, *Hoxa11eGFP* expression is observed in much of the large callus formed around the fracture site (Figure 3.2A). Notably, *Hoxa11eGFP* positive cells are not observed in the central cartilage region of the callus but are observed largely at the interface between cartilage and mineralization zones (Figure 3.2A). *Hoxa11eGFP* is also

Figure 3.2

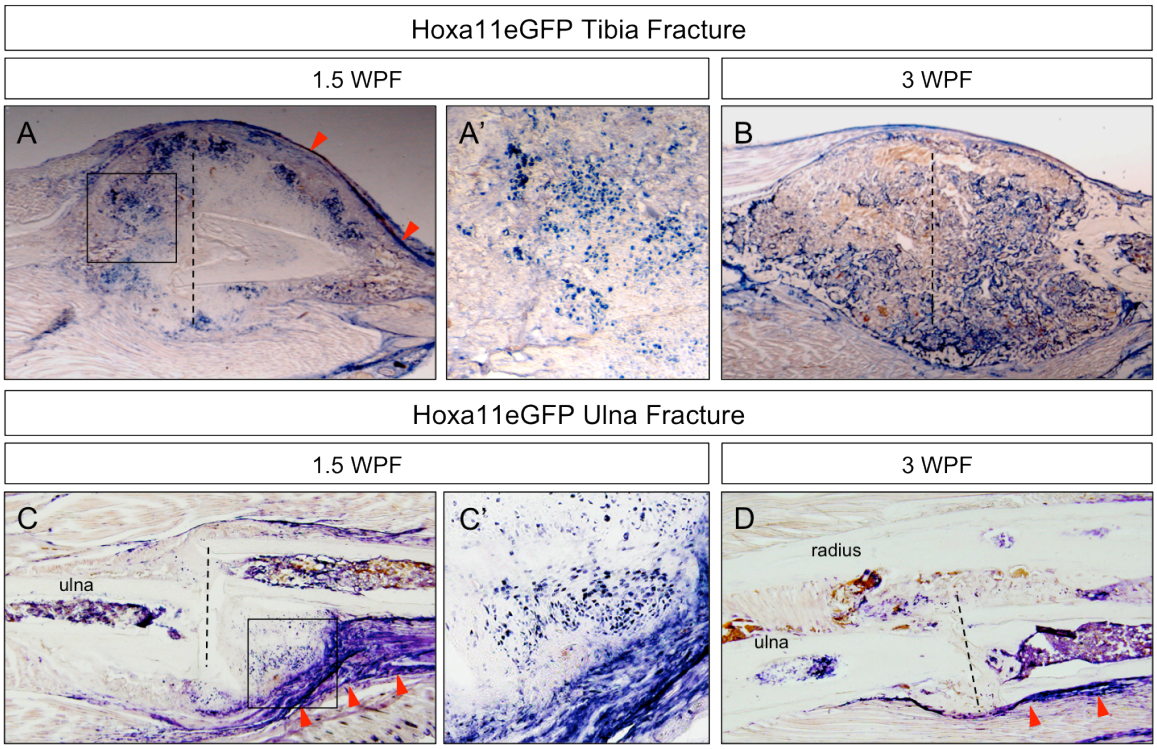

Figure 3.2. *Hoxa11eGFP* expression is up-regulated during skeletal repair. *Hoxa11eGFP* was detected by antibody stain for GFP in sections of *Hoxa11eGFP* heterozygous limbs following tibia fracture (A, B) or ulna fracture (C, D). At 1.5 weeks post fracture (WPF) in the tibia and ulna, *Hoxa11eGFP* is expressed highly in the distal periosteal region (A, C, red arrowheads). The 1.5 WPF fracture callus also shows strong *Hoxa11* expression (A, A', C, C'). *Hoxa11eGFP* expression is observed periosteally and on the surfaces of woven bone at 3 WPF (B, D).

strongly expressed in the distal periosteum (Figure3.2A, red arrowheads). The callus in the ulnar fracture model is significantly smaller than the tibial fracture callus but shows similar *Hoxa11eGFP* expression patterns. *Hoxa11eGFP* is expressed in cells around the periphery of the callus at 1.5 WPF (Figure 3.2C). There is also strong expression of *Hoxa11eGFP* in the periosteum following ulna fracture (Figure 3.2C, D, red arrowheads).

At 3 WPF, the cartilage template has been largely replaced by mineralized matrix (Schindeler et al., 2008; Ushiku et al., 2010). Osteoclasts are recruited to remodel the bone callus and to reestablish the original cortical and trabecular architecture (Väänänen and Laitala-Leinonen, 2008). At 3 WPF in the tibial fracture model, *Hoxa11eGFP* is expressed strongly throughout the entire callus in cells along the surfaces of the remodeling bone (Figure 3.2B). Scattered *Hoxa11eGFP* positive cells are observed in the ulna callus during this remodeling phase (Figure 3.2D).

During the early, soft callus phase of fracture healing a large component of the callus is cartilage. Cartilage functions to stabilize and provide strength to the fracture. Safranin-O stains the proteoglycan-containing matrix of the cartilage. We found that *Hoxa11eGFP* is expressed in regions of the callus that do not stain for Safranin-O as well as within some parts of the Safranin-O positive cartilage (Figure 3.3A). Staining with the early chondrocyte marker Sox9 shows that *Hoxa11eGFP* is most strongly expressed in the cells adjacent to the Sox9 expressing differentiating chondrocytes on the periphery of the callus (Figure 3.3B). There is some coexpression of *Hoxa11eGFP* and Sox9, largely in cells at the boundary between these two expression domains (Figure 3.3B). The

Figure 3.3

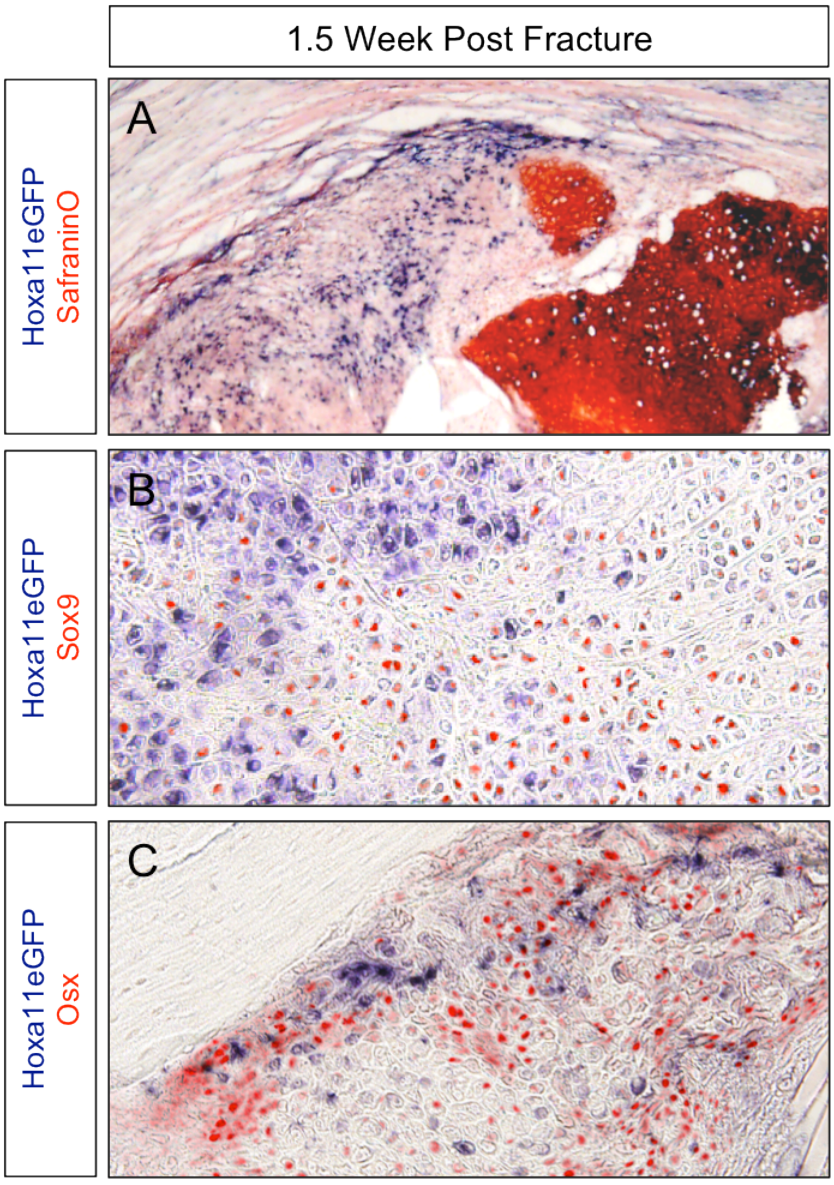

Figure 3.3. *Hoxa11eGFP* expression in the fracture callus is largely excluded from differentiating chondrocytes and osteoblasts. Sections of tibial fractures at 1.5 WPF (A-C). Staining for *Hoxa11eGFP* and the cartilage stain Safranin-O (A) shows that *Hoxa11* is expressed in areas of mature cartilage and also in regions that do not stain with Safranin-O. Antibody stain for the chondrocyte marker *Sox9* (B) shows *Hox11* expressing cells are adjacent to *Sox9* expressing chondrocytes. A few cells in the transition zone appear to express both markers at low levels. *Hoxa11eGFP* is mainly excluded from cells expressing the early osteoblast marker Osx (C).

position of the *Hoxa11eGFP*-positive cells relative to Safranin-O and Sox9 suggests that at least a subpopulation of *Hoxa11eGFP* cells may be of the chondrocyte lineage.

Osteoblasts also begin to invade the callus at the soft callus stage and form new bone from the periphery of the callus. Staining with an antibody for the early osteoblast marker Osterix (Osx) shows that *Hoxa11eGFP* is excluded from osteoblasts within the fracture callus (Figure 3.3C).

Hox11 compound mutant mice show alterations in callus morphology and fracture healing is impaired

The levels of *Hox11* expression after fracture injury suggested a possible role for these genes in healing. To assess the functional role of *Hox11* genes in fracture healing, we performed ulnar fractures in *Hox11* compound mutant mice. Mice used in this study have three of the four active *Hox11* alleles mutated. These mice provide a genetic model of reduced *Hox11* function that still permits relatively normal skeletal patterning.

To determine whether the loss of *Hox11* function alters fracture healing, we examined ulnar fractures of control and *Hox11* compound mutants by radiograph and high-resolution microCT at 1.5, 3, 6, and 12 weeks post injury. Radiographs show a defect in mineralized bridging across the fracture gap in Hox11 compound mutants compared to controls (Figure 3.4). MicroCT images show notable differences by 3 WPF between controls and mutants. *Hox11* compound mutants fail to form mineralized material across the fracture gap as observed in controls at this stage (Figure 3.5C, D). This incomplete mineralized bridging remains at 6 WPF, a time point at which controls have reformed a smooth cortical surface (Figure 3.5E, F). By 12 WPF, both control and

Hox11 compound mutants appear to have externally remodeled to form a smooth surfaced bone (Figure 3.5G, H), although more detailed analyses below show the mutants havbe not yet remodeled completely.

MicroCT also allowed us to precisely measure the callus volume, bone volume, bone volume fraction (BVF), bone mineral content (BMC), and tissue mineral density of healing ulna fractures and unfractured 8 week old control and *Hox11* compound mutant mice. The only statistically significant differences were observed in the unfractured animals and at 12 weeks post fracture. *Hox11* compound mutants have increased ulna size and decreased BVF compared to controls (Table 3.1). While the size of the *Hox11* compound mutant callus did trend to be larger, this was only statistically significant at 12 WPF (Table 3.1). At this stage, the BMC was also increased in *Hox11* compound mutants (Table 3.1). The region of interest used for these analyses includes new callus bone and original cortical bone. As we observed significant differences in the unfractured *Hox11* bone, it is likely that the original cortical bone included in these results may be masking any differences observed in new callus formation. Further analysis of microCT data after separation of original cortical bone from newly formed callus bone may reveal differences in mineralization properties between control and *Hox11* compound mutants and will be performed in future experiments.

Hox11 compound mutant mice show a reduction in callus cartilage

One of the first and most important defects an animal must overcome after skeletal fracture is the instability caused by injury. Most fractures display some level of mechanical instability and heal partially by re-employing endochondral ossification, in

Figure 3.4

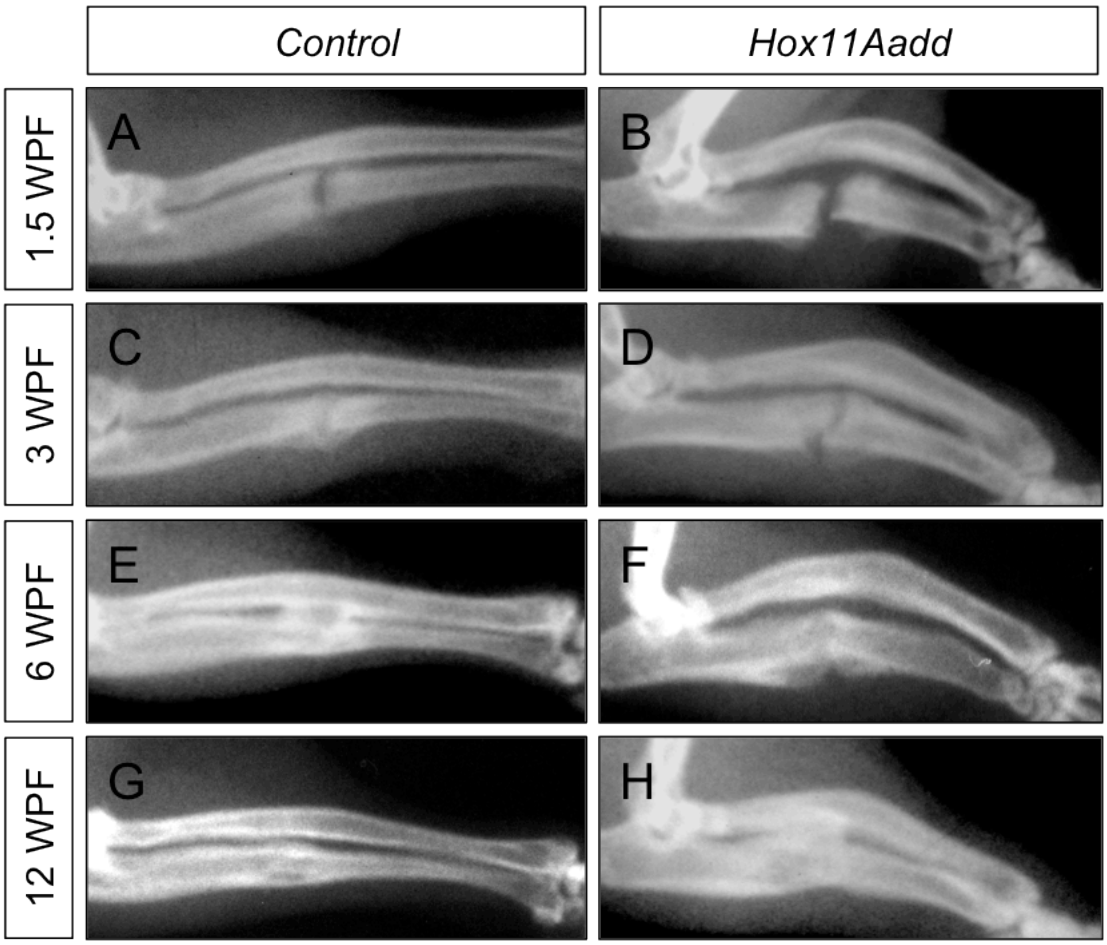

Figure 3.4. Skeletal healing of *Hox11* compound mutant ulnar fracture is impaired. Radiographs of control (A, C, E, G) and *Hox11* compound mutant (B, D, F, H) ulnar fractures. There is an apparent defect in mineralization in *Hox11* mutants from 3 WPF on (C-H).

Figure 3.5

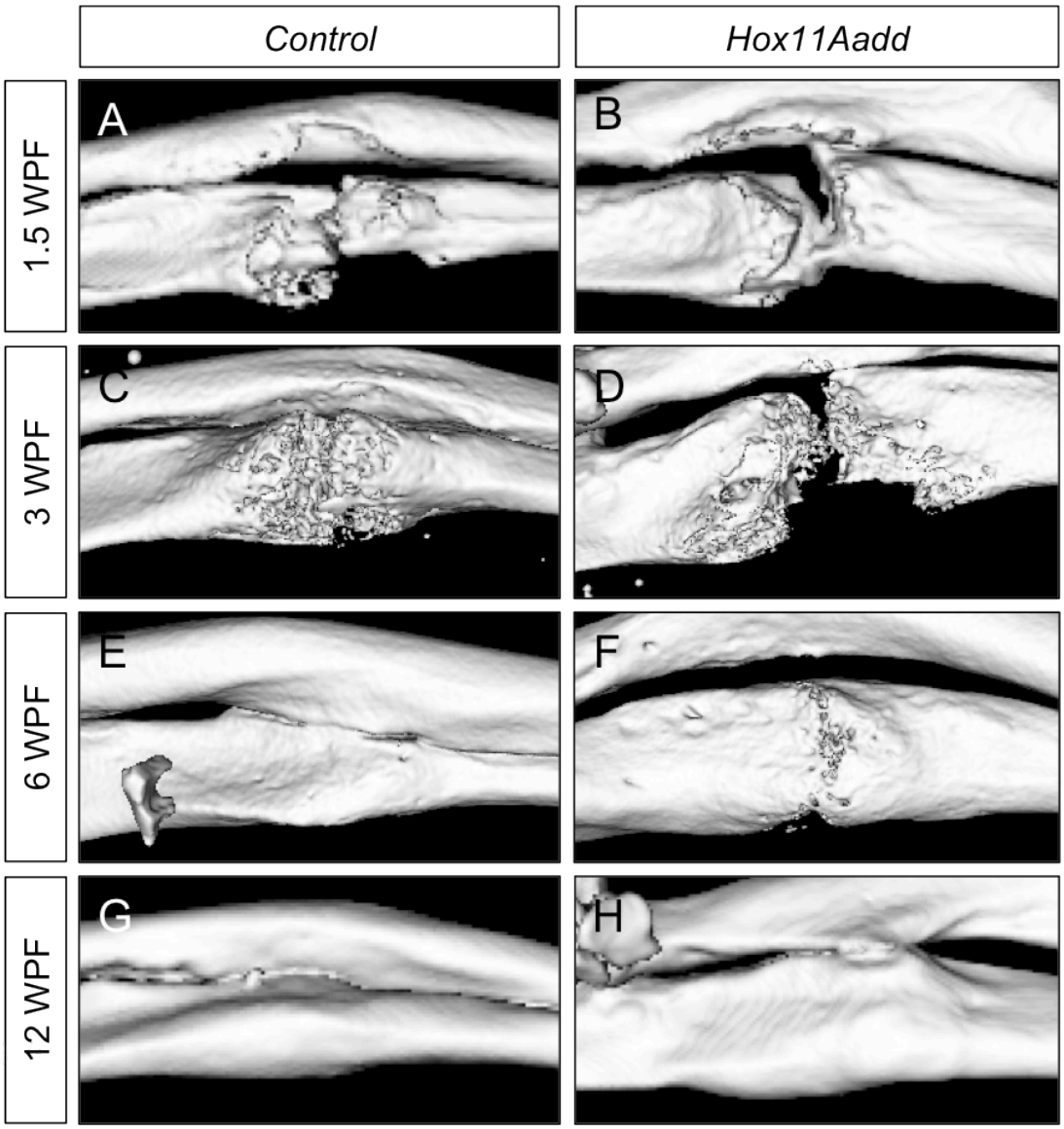

Figure 3.5. Skeletal repair is impaired in *Hox11* compound mutants. Representative isosurface renderings of μCT scans of wild type control (A, C, E, G) and *Hox11* compound mutant (B, D, F, H) ulna fractures. At 1.5 WPF no differences are observed between control and *Hox11* compound mutants (A, B). At 3 WPF, *Hox11* compound mutants have a visible gap at the fracture site while control animals have mineralized tissue filling the entire fracture gap at this stage (C, D). At 6 WPF, controls have completely mineralized across the fracture to form smooth cortical bone but significant unmineralized area remains in compound mutants (E, F). Both control and *Hox11* compound mutants are healed by 12 WPF (G, H).

Table 3.1

Measured Parameter	*Unfractured*		*1.5 weeks post fracture*		*3 weeks post fracture*	
	Control (n=4)	*Hox11Aadd (n=8)*	*Control (n=5)*	*Hox11Aadd (n=8)*	*Control (n=5)*	*Hox11Aadd (n=6)*
Total Volume (mm^3)	0.43 (0.01)	0.53 (0.04)*	1.81 (0.45)	2.53 (0.92)	1.74 (0.22)	1.59 (0.50)
Bone Volume (mm^3)	0.31 (0.01)	0.35 (0.03)*	0.52 (0.13)	0.74 (0.22)	0.57 (0.08)	0.57 (0.21)
Bone Volume Fraction (%)	0.72 (0.01)	0.67 (0.02)*	0.32 (0.18)	0.31 (0.09)	0.33 (0.05)	0.35 (0.05)
BMC (mg)	0.36 (0.01)	0.39 (0.05)	0.82 (0.14)	1.02 (0.32)	0.89 (0.08)	0.78 (0.31)
Tissue Mineral Density (mg/ml)	994.2 (22.4)	905.6 (85.4)	935.3 (101.8)	877.5 (105.3)	838.0 (31.3)	792.5 (74.3)

Measured Parameter	*6 weeks post fracture*		*12 weeks post fracture*	
	Control (n=5)	*Hox11Aadd (n=6)*	*Control (n=5)*	*Hox11Aadd (n=4)*
Total Volume (mm^3)	1.45 (0.25)	1.61 (0.62)	0.99 (0.12)	1.52 (0.27)*
Bone Volume (mm^3)	0.79 (0.13)	0.81 (0.28)	0.63 (0.10)	0.93 (0.04)*
Bone Volume Fraction (%)	0.55 (0.07)	0.51 (0.05)	0.64 (0.04)	0.63 (0.09)
BMC (mg)	0.95 (0.17)	0.97 (0.34)	0.79 (0.13)	1.23 (0.07) *
Tissue Mineral Density (mg/ml)	896.8 (48.6)	866.9 (37.1)	1036.2 (26.4)	1054.0 (72.6)

Table 3.1. μCT parameters of harvested fractures. For statistical analysis control was compared with *Hox11* compound mutant at the indicated time point. *$p<0.05$.

which a cartilage template forms to stabilize the fracture and is later replaced by bone. To assess the level of cartilage produced by mutant compared to control after fracture, callus sections were stained with Safranin-O. Qualitatively, a reduction in cartilage can be observed in *Hox11* compound mutants at 1.5 WPF (Figure 3.6A, E), 3 WPF (Figure 3.6B, F) and 6 WPF (Figure 3.6C, G). By 12 WPF, no cartilage is present in control or mutant fractures (Figure 3.6G, H). The fracture callus of *Hox11* compound mutants have not remodeled woven bone even as late as at 12 WPF whereas control animals have mainly re-attained normal cortical bone morphology by this stage (Figure 3.6G, H). Quantification of the percentage of Safranin-O positive cartilage using histomorphometry, reveals that *Hox11* compound mutants have a significant reduction in mature cartilage matrix after fracture (Figure 3.6I). These data suggest that *Hox11* function is necessary to promote cartilage formation or maturation in the fracture callus.

Osteoclasts are present in *Hox11* compound mutant callus

Our preliminary results show compelling evidence that *Hox11* is strongly expressed during the hard callus stage, and in regions that are lining the new osteal surfaces; the same regions where osteoclasts localize at this stage. *Hox11* compound mutants also show an apparent delay in remodeling compared to controls. These data are consistent with a role for *Hox11* genes in osteoclast differentiation and/or function during skeletal repair and remodeling. To examine the possible difference in osteoclast formation, we stained for TRAP in the fracture callus at 3, 6, and 12 WPF in control and compound mutants. No obvious differences in TRAP staining were observed at 3 and 6 WPF (Figure 3.7A-D). At 12 WPF, control animals have largely completed remodeling

Figure 3.6

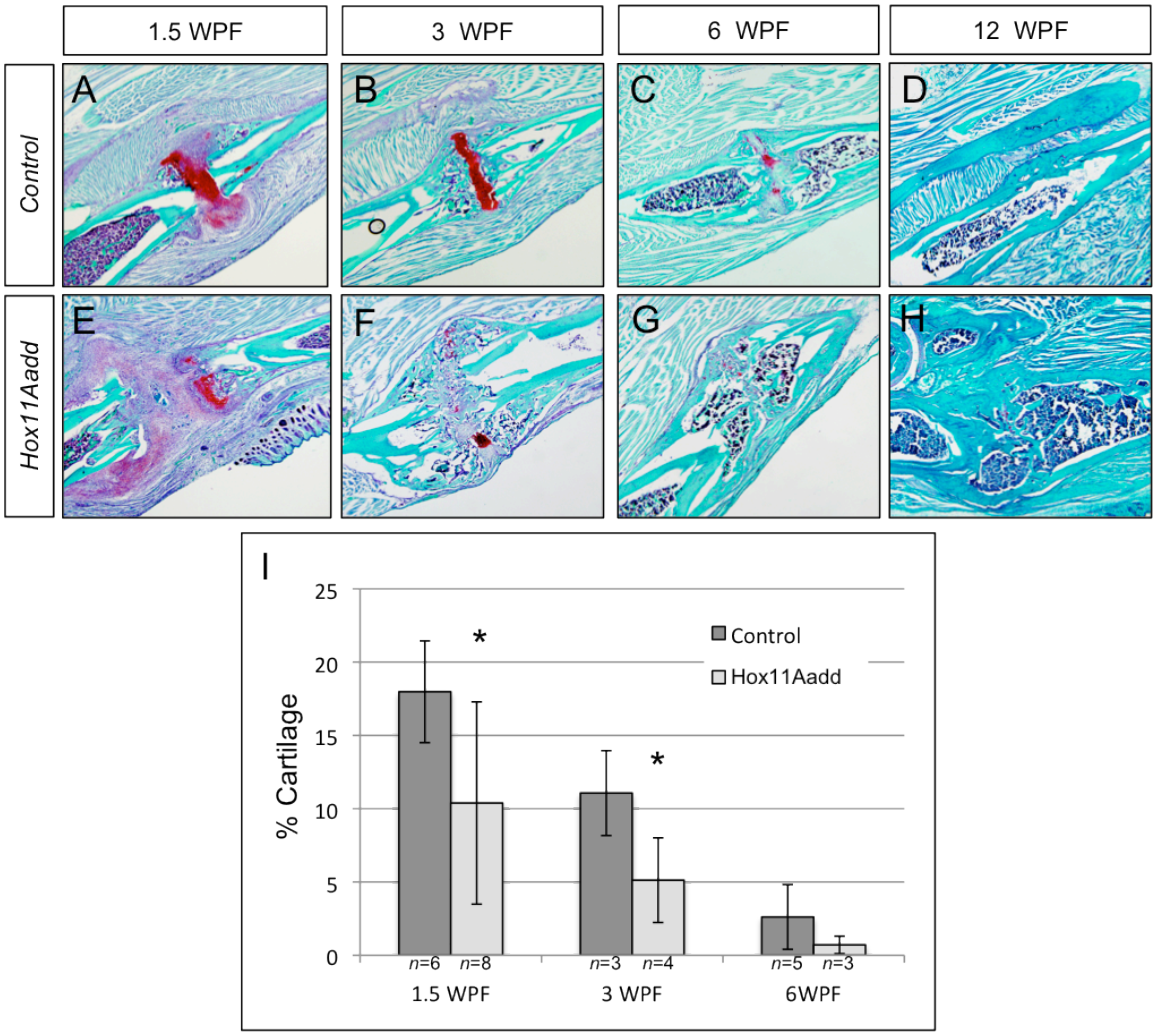

Figure 3.6. *Hox11* compound mutant mice produce less cartilage in response to fracture injury than controls. Mid-callus sections stained with Safranin-O/Fast Green (A-H). Red Safranin-O staining is proteoglycan-containing cartilage. Controls show intense Safranin-O staining at the fracture gap that decreases as repair proceeds (A-D). Hox11 compound mutants form less cartilage than control (E-H). No cartilage is present in control or *Hox11* compound mutant callus at 12 WPF (D, H). The percentage of the callus that is cartilage is significantly reduced in *Hox11* compound mutants compared to controls (I). *Statistical significant differences ($p<0.05$).

Figure 3.7

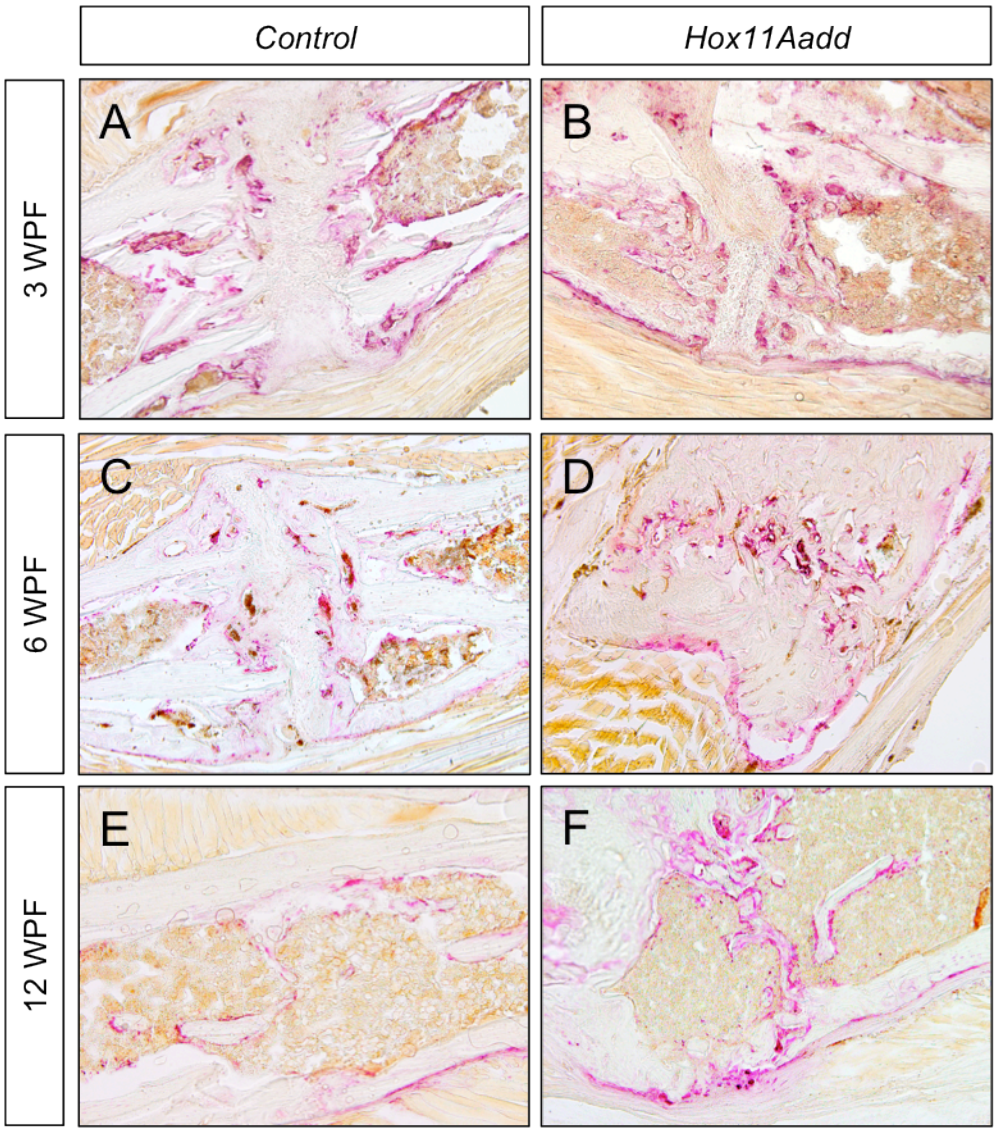

Figure 3.7. Loss of *Hox11* does not affect osteoclast formation as measured by TRAP staining. Mid-callus sections stained for Tartrate Resistant Acid Phosphatase (TRAP) to mark osteoclasts shows that *Hox11* compound mutants (B, D) have similar numbers of TRAP staining cells compared to controls (A, C) at 3 and 6 WPF. While there is a decrease in the number of TRAP positive cells in controls by 12 WPF, this decrease is not observed in *Hox11* mutants (E, F).

and TRAP staining appears to have decreased significantly, however, in *Hox11* compound mutant high numbers of TRAP positive cells are still observed, consistent with remodeling being incomplete at this stage (Figure 3.7E, F). These data suggest that loss of *Hox11* does not affect osteoclast formation but does not rule out a potential defect in osteoclast function.

DISCUSSION

Extensive genetic analyses demonstrate the importance of *Hox* genes in patterning along the AP axis of the body and the PD axis of the limb during embryonic development (Chisaka and Capecchi, 1991; Davis et al., 1995; Fromental-Ramain et al., 1996b; Kmita et al., 2005; McIntyre et al., 2007; Wellik, 2007; Wellik and Capecchi, 2003; Wellik et al., 2002; Zakany et al., 2007). Recent studies suggest that at least parts of the *Hox* code are maintained throughout adult life and may play roles in providing patterning information during homeostasis and repair (Ackema and Charité, 2008; Chi et al., 2007; Gesta et al., 2006; Leucht et al., 2008; Rinn et al., 2006; Rinn et al., 2008). Here we report that *Hox11* genes are regionally expressed in skeletal tissues throughout postnatal and adult stages in a pattern reminiscent of their developmental expression. We also observed substantial increases in cells expressing *Hox11* in the fracture callus during skeletal repair. These data led us to examine whether *Hox* genes have a continued function in skeletal remodeling and healing. In fact, we observed a significantly impaired fracture healing response in *Hox11* compound mutant fractures compared to controls.

Our results show that *Hox11* expression is maintained in the periosteum and endosteum of the distal radius and ulna throughout postnatal and adult stages. The

periosteum and endosteum are important tissues for skeletal remodeling and repair. The periosteum is composed of fibroblasts, osteoblasts and undifferentiated mesenchymal stem cells. During fracture repair, the periosteum serves as a reservoir for stem cells that are able to differentiate into chondrogenic and osteoblastic lineages (Ito et al., 2001; Malizos and Papatheodorou, 2005; Tamer and Reis, 2009). Therefore *Hox11* expression within this tissue may be critical for healing and remodeling of bone.

In the fracture gap, mesenchymal cells differentiate to become either osteoblasts or chondrocytes (Schindeler et al., 2008). Our analysis of *Hox11* compound mutant fractures shows a reduction in cartilage percentage within the callus, consistent with differences in chondrocyte differentiation or maturation. Previous studies of limb development in *Hox11* mutant mice have shown that chondrocyte specification occurs normally, however, maturation of chondrocytes to hypertrophy is defective (Boulet and Capecchi, 2004). Further experiments are needed to address the maturation state of chondrocytes within the *Hox11* compound mutant fracture callus.

Mechanical stability is a crucial component that can significantly influence the cellular events of healing and the resultant callus phenotype. A possible caveat of this study is mechanical differences that may exist between *Hox11* compound mutant and control ulnar fractures due to the skeletal phenotype of *Hox11* compound mutant forelimbs. By adult stages, the radius and ulna of *Hox11* compound mutant animals are shorter than control animals (Davis et al., 1995). In addition, the ulna of *Hox11* compound mutants remains straight while the radius curves anteriorly (Davis et al., 1995). The curvature of the radius may place additional mechanical force on the ulna following fracture. While additional mechanical forces would lead to a prediction of

increased cartilage formation, not less, we plan to address this caveat by generating a *Hoxd11* conditional allele that will allow for inactivation of *Hox11* after skeletal growth is complete. This will allow an assessment of role of *Hox11* in fracture repair separate from its role in growth and development.

We have observed reduced cartilage formation and impaired mineralization across the fracture gap, demonstrating that *Hox11* is critical for establishing appropriate callus architecture to support bone healing. These data show that regionally restricted *Hox* genes are important not only for initial tissue patterning and morphogenesis but also healing and repair processes.

MATERIALS AND METHODS

Mice

All procedures followed protocols reviewed and approved by the University of Michigan's Committee on Use and Care of Animals. The mice used for *Hox11* expression analysis were heterozygous for the *Hoxa11eGFP* targeted knock-in, knock-out allele (Nelson et al., 2008). Compound mutants of *Hoxa11* and *Hoxd11* null alleles were generated by traditional breeding strategies (Boulet and Capecchi, 2004). Coisogenic wild type mice were used for comparison.

Surgical Procedures

We created closed, transverse fractures in the left tibia of 8-10 week old mice following methods similar to those described by Hiltunen et al (Hiltunen et al., 1993). Briefly, mice were anesthetized for all surgical procedures using isoflurane and the left

leg was prepared for aseptic surgery. The stifle joint of the leg was flexed and a small incision was made just medial to the tibial tuberosity. A 26-guage hypodermic needle was used to bore a hole in the cortex of the medial aspect of the tibial Tuberosity and a sterile, 0.009-in-diameter, stainless steel pin was inserted down the length of the tibia intramedullary canal. This served to provide stability to the fracture site. After pin insertion, the pin was cut to be flush with the cortex and the skin was closed using tissue adhesive. Fractures were created using a custom-made device that uses a sliding weight and guillotine mechanism to provide consistent, high-energy impact force sufficient to induce fracture. Post-operative radiographs were taken to verify pin placement and fracture gap location. Mice were provided chow and water ad libitum following the procedure and were typically ambulatory within 1 hr after surgery.

For ulna fractures, mice were anesthetized with isoflurane, and a small incision was made along the posterior surface of the ulna. The mid-ulnar diaphysis was exposed via blunt dissection through the overlying soft tissues, and using a fine wire cutter, was cut at the mid-shaft. The radius was left intact to provide stability to the fracture. Skin was closed with skin glue, and post-operative radiographs were taken to ensure cut ends remained closely apposed. All animals were fully weight bearing within 30 minutes following surgery, and were given chow and water ad libitum until the time of euthanasia.

Histology, immunohistochemistry and histomorphometric measurements

Limbs were collected at the appropriate time points following fracture surgery and intramedullary pins were removed if present. All specimens were dissected in PBS on ice and scanned immediately for μCT and then fixed for 3 days in 4%

paraformaldehyde in PBS at 4°C. Limbs were then decalcified in 14% EDTA for one week prior to embedding into OCT media. Cryosections were collected at 16 μm through the entire fracture callus. Immunohistochemical staining was performed using antibodies for Sox9 (1:500, Millipore, AB5535), Osx (1:1000, Abcam, ab22552). To minimize complications resulting from high autofluorescence in adult tissues we used an antibody to GFP (1:500, Invitrogen, A-11122) followed with an alkaline phosphatase conjugated secondary antibody (1:500, Jackson ImmunoResearch, 111-055-003) for all analysis of *Hoxa11eGFP* expression. TRAP staining was performed using a leukocyte acid phosphatase kit (Sigma).

To determine the amount of cartilage within each callus, every 10th section was stained with Safranin-O/Fast Green/Hematoxylin as previously described (Thompson et al., 2002). Images were captured on an Olympus BX-51 upright light microscope at 10X magnification with an Olympus DP70 camera. The area of callus and cartilage on each section was determined using ImageJ software (Schneider et al., 2012). Using the manual measure function of this software, we identified appropriate areas of the entire callus and Safranin-O stained regions and outlined them. A minimum of three tissue sections per callus were measured and the average was calculated.

μCT analyses

Samples were scanned using an eXplore Locus SP microCT system (GE Healthcare). All specimens were scanned in water using the following parameters: voltage 80 kVp; current 80 μA; exposure time 1600 ms; voxel size in the reconstructed image 10 μm, isotropic. The data were processed and analyzed using MicroView (v

2.1.2 Advanced Bone Application; GE Healthcare Preclinical Imaging). First, the image was reoriented so that the anterior-posterior and longitudinal axes were aligned with the principal image axes. Next, the callus was manually segmented starting with a frame at the center of the fracture and extending 72 μm on either side to identify a 144 μm region of interest. The callus volume, bone volume, bone volume fraction, bone mineral content (BMC), and tissue mineral density (TMD) were calculated. These measurements include callus and original cortical bone.

ACKNOWLEDGEMENTS

I would like to thank Dr. Steve Goldstein and Dr. Kenneth Kozloff and the University of Michigan Orthopedic Research Laboratories for their assistance with fracture surgeries and comments and suggestions. I would also like to acknowledge Alyssa Lau and Danielle R. Rux for their contributions to this chapter.

CHAPTER IV

CONCLUSION

Summary of findings

Previous to the work reported in this thesis, genetic analyses of *Hox* loss-of-function skeletal phenotypes have demonstrated that these genes are essential regulators of skeletal patterning during development. However, as studies of *Hox* function in limb development have been limited to the skeleton, our understanding of the cell types in which *Hox* genes function and the tissues they pattern is incomplete. We report here the first in-depth analysis of *Hox11* expression and function throughout limb development as well as adult fracture repair to further understand how these genes may function during morphogenesis.

Our data demonstrate that *Hox11* genes play a more extensive role in musculoskeletal patterning and repair than previously appreciated. Previous research has demonstrated that *Hox11* genes are critical for the morphogenesis of zeugopod skeletal elements. We revealed that *Hox11* genes are also essential for the patterning of the soft tissue components of the musculoskeletal system within the limb zeugopod. In the absence of *Hox11*, muscle and tendon patterning in this region is dramatically disrupted while other limb regions are largely unaffected.

Our analysis of *Hox11* expression reveals that *Hox11* genes are expressed broadly in the limb mesenchyme at early stages but are excluded from Sox9-expressing chondrocytes within the developing skeletal elements. *Hox11* expression is observed throughout the remainder of limb development in the perichondrium surrounding skeletal elements as well as in tendons and muscle connective tissue. Previous reports have focused on the early, broad expression of Hox genes during limb development (Cohn et al., 1997; Haack and Gruss, 1993; Hostikka and Capecchi, 1998; Izpisúa-Belmonte and Duboule, 1992); however, our findings suggest that *Hox* genes are likely to play a continued role in tissue morphogenesis and growth throughout development. In addition, we have observed that *Hox11* expression is maintained throughout postnatal and adult stages suggesting that these genes function well beyond the initial tissue patterning events.

Consistent with the idea that *Hox* function is required beyond embryogenesis, our results demonstrate that *Hox11* expression is up-regulated during fracture repair. *Hox11* is expressed in cells around the periphery of the fracture callus at 1.5 weeks post fracture during the soft callus phase of healing. Functionally, we have shown that loss of *Hox11* results in impaired fracture healing. In *Hox11* compound mutant fractures, a reduction of cartilage is observed suggesting that *Hox* may regulate the maturation of cartilage during the repair process, similar to its developmental role. Details of *Hox* function in fracture repair continue to be a focus of the Wellik laboratory.

Implications

The study of *Hox* loss-of-function and gain-of-function skeletal phenotypes has inspired the idea that *Hox* genes are important regulators in modifying the animal body plan during evolution. Our findings show that *Hox11* genes are involved in the regional patterning of multiple tissue components that shape the limb zeugopod musculoskeletal system. Other *Hox* paralogous groups function to shape skeletal elements in different regions of the limb. For example, *Hox9* and *Hox10* genes are required for stylopod development and *Hox13* genes function in the autopod (Fromental-Ramain et al., 1996a; Fromental-Ramain et al., 1996b; Wellik and Capecchi, 2003). It is likely that these paralogs function in a similar way to *Hox11* to integrate the musculoskeletal system in their specific expression domains. This study expands our understanding of how *Hox* genes function to instruct the body plan.

This work also raises the question of how *Hox* genes might function in patterning muscle and tendon along the body axis. Studies of Hox paralogous mutants have shown that these genes control skeletal patterning of anatomical axial domains (Mallo et al., 2010; McIntyre et al., 2007; Wellik and Capecchi, 2003). Do *Hox* genes also pattern the associated muscle and tendon in these regions? Our work has shown that *Hox11* is expressed throughout connective tissues of the perichondrium, tendons and muscle connective tissue in the limb. Is connective tissue also an important cell population for *Hox* patterning in the axial skeleton?

This research also brings attention to the continued role of *Hox* genes throughout the life of the organism. Not only is *Hox11* expressed through late embryonic stages, this expression is maintained through postnatal and adult life. Our demonstration that *Hox11*

genes function in fracture healing reveals a continued critical role for these genes after development. Our combined data suggest the interesting possibility that, *Hox* genes function continuously in the adult animal to impart morphogenetic information to specific anatomical regions. This has important implications for the field of regenerative medicine. *Hox* expression status may be an important feature of grafted cells that could determine the success or failure of these types of treatments.

Future Directions

The work described here has raised many questions about how *Hox* genes regulate complex patterning events in multiple tissues. There is much left to be learned about *Hox* function in development, tissue maintenance and regeneration and repair.

We have identified connective tissue fibroblasts as an important cell population that express *Hox11* throughout musculoskeletal development. This opens the possibility for further analyses of this cell type to assess the cellular and molecular mechanisms of *Hox* function. Morphogenesis relies on the coordinated action of numerous cellular events such as cell migration, proliferation, cell adhesion, and cell shape changes. Studying the effect of *Hox* loss-of-function on these cellular behaviors *in vitro* may provide important insights into the mechanisms by which *Hox* directs patterning events *in vivo*. *In vitro* culture of *Hox11* mutant fibroblasts will also allow us to assess their ability to respond to growth factors, remodel extracellular matrix, respond to other cells in a culture environment, and other cellular behaviors.

Our analysis of *Hoxa11eGFP* demonstrates that *Hox11* expression is excluded from the skeletal elements from early stages of development; however, these results

cannot determine if *Hox11*-expressing cells can give rise to chondrocytes or osteoblasts. The ideal method to ascertain the fate of *Hox11* cells would be to perform lineage-tracing experiments to genetically mark the *Hox*-expressing cells and their progeny to determine the differentiation of these cells. An alternative approach is isolation of *Hox11eGFP* positive cells followed by assessment of their potential to differentiate into chondrocyte or osteoblast lineages.

As *Hox11* expression is also observed throughout developmental stages as well as postnatal growth and adult life, the question of when *Hox* genes function to regulate patterning, growth and repair becomes significant. When does the initial patterning occur and when are these patterning events complete? Current work in the lab is focused on generating a *Hoxd11* conditional allele that will allow us to address the timing of *Hox* function. Conditional inactivation of *Hox11* genes during stages of musculoskeletal development will allow a more precise determination of the requirement of *Hox11* function for muscle, tendon and skeletal patterning events.

We have observed *Hox11* expression in postnatal and adult stages and determined that *Hox11* genes have a functional role in fracture healing. However, the function of *Hox* genes in adult skeletal tissues in the absence of injury is unknown. Are *Hox* genes necessary for normal skeletal homeostasis? To begin to address this important question our lab is analyzing the expression of *Hox11* in adult mice to determine the particular cell types in which these genes are expressed. We are also performing a detailed analysis of the postnatal and adult skeletal phenotype of *Hox11* compound mutant animals to elucidate the role of these genes in growth and adult life. By conditionally inactivating

Hox11 expression at adult stages after skeletal growth is complete we will be able to separate developmental effects of *Hox* inactivation from their role skeletal homeostasis.

The work described here has begun to examine the cell types that express *Hox11* following fracture injury; however, we have not been able to precisely identify all of the *Hox11*-expressing cell populations within the fracture callus. Continued analysis is focused on indentifying other *Hox11*-expressing cell types following fracture injury.

During limb development, *Hox11* gene expression is largely restricted to the limb zeugopod region. *Hox9* and *Hox10* genes function in the stylopod and *Hox13* genes are required for autopod development. Our results show that *Hox11* expression in the zeugopod is maintained in postnatal and adult stages. *Hox11* is also expressed highly after fracture injury in the zeugopod region. We hypothesize that *Hox9* and *Hox10* genes will be required for fracture healing in the stylopod region and *Hox11* will not be expressed in a fracture at this location. Our lab is performing femur fracture experiments using *Hoxa11eGFP* animals to assess the expression of *Hox11* genes following fracture of the stylopod region. To determine the functional requirement for *Hox* genes within these specific limb regions, we can perform transplant experiments. In these experiments, a skeletal graft from one limb region is transplanted into a skeletal defect in another limb region. For example, a *Hox11* positive graft from the zeugopod could be transplanted into the *Hox9*/*10* positive stylopod region allowing us to evaluate the region-specific functions of these genes in healing. Understanding how *Hox* expression status could influence healing potential may be very valuable to tissue engineering and regenerative medicine.

Our ultimate goal is to elucidate the downstream targets and pathways in which *Hox* genes operate. Identifying *Hox* target genes has proven elusive for multiple reasons. All *Hox* proteins contain a highly-conserved DNA binding domain called the homeodomain that recognizes the same ATTA DNA element (Svingen and Tonissen, 2006). Further, many *Hox* genes act as repressors or activators of target genes depending on developmental context. In an effort to identify *Hox* targets in limb development we performed microarray analysis on *Hoxa11eGFP* positive cells from control and *Hox11* double mutant limbs. This analysis yielded interesting potential targets involved in skeletal system development, as was expected, but also cell adhesion, cell migration and extracellular matrix structure and organization. Ongoing work in the laboratory is focused on confirming potential target genes.

In conclusion, our work has provided valuable insights into *Hox* gene function. Our data show that *Hox* genes are not only critical skeletal patterning factors but regulate the morphogenesis of muscle, tendon and bone to form an integrated musculoskeletal system. In addition, *Hox* genes have roles beyond initial development and patterning events to direct repair processes during adult life.

APPENDIX

ADDITIONAL PUBLICATIONS

During the course of my project I contributed to the following additional publications that are not included in the primary work of my thesis:

Ma, J, Smietana, MJ, **Swinehart, IT**, Kostrominova, TY, Wellik, DM, Wojtys, EM, Larkin, LM, Arruda, EM "A comparison of tissue engineered scaffold-less bone-ligament-bone constructs and patellar tendon autografts used for anterior cruciate ligament replacement in sheep." Under revision for publication in American Journal of Sports Medicine.

Yallowitz AR*, Gong K-Q*, **Swinehart IT**, Nelson LT, and Wellik, DM (2009). "Non-homeodomain regions of Hox proteins mediate activation versus repression of Six2 via a single enhancer site in vivo ". Developmental Biology 335(1):156-165.
*Co-first authors

COMPLETE REFERENCES

Ackema, K. B. and Charité, J. (2008). Mesenchymal stem cells from different organs are characterized by distinct topographic Hox codes. *Stem Cells Dev.* **17**, 979–991.

Axelrad, T. W., Kakar, S. and Einhorn, T. A. (2007). New technologies for the enhancement of skeletal repair. *Injury* **38 Suppl 1**, S49–62.

Baksh, D., Song, L. and Tuan, R. S. (2004). Adult mesenchymal stem cells: characterization, differentiation, and application in cell and gene therapy. *J. Cell. Mol. Med.* **8**, 301–316.

Bandyopadhyay, A., Kubilus, J. K., Crochiere, M. L., Linsenmayer, T. F. and Tabin, C. J. (2008). Identification of unique molecular subdomains in the perichondrium and periosteum and their role in regulating gene expression in the underlying chondrocytes. *Dev Biol* **321**, 162–174.

Blitz, E., Viukov, S., Sharir, A., Shwartz, Y., Galloway, J. L., Pryce, B. A., Johnson, R. L., Tabin, C. J., Schweitzer, R. and Zelzer, E. (2009). Bone ridge patterning during musculoskeletal assembly is mediated through SCX regulation of Bmp4 at the tendon-skeleton junction. *Dev Cell* **17**, 861–873.

Bolander, M. E. (1992). Regulation of fracture repair by growth factors. *Proc. Soc. Exp. Biol. Med.* **200**, 165–170.

Bonnin, M.-A., Laclef, C., Blaise, R., Eloy-Trinquet, S., Relaix, F., Maire, P. and Duprez, D. (2005). Six1 is not involved in limb tendon development, but is expressed in limb connective tissue under Shh regulation. *Mech Dev* **122**, 573–585.

Boulet, A. M. and Capecchi, M. R. (2002). Duplication of the Hoxd11 gene causes alterations in the axial and appendicular skeleton of the mouse. *Dev Biol* **249**, 96–107.

Boulet, A. M. and Capecchi, M. R. (2004). Multiple roles of Hoxa11 and Hoxd11 in the formation of the mammalian forelimb zeugopod. *Development* **131**, 299–309.

Bruder, S. P., Fink, D. J. and Caplan, A. I. (1994). Mesenchymal stem cells in bone

development, bone repair, and skeletal regeneration therapy. *J Cell Biochem* **56**, 283–294.

Buckingham, M., Bajard, L., Chang, T., Daubas, P., Hadchouel, J., Meilhac, S., Montarras, D., Rocancourt, D. and Relaix, F. (2003). The formation of skeletal muscle: from somite to limb. *J Anat* **202**, 59–68.

Busse, J. W., Bhandari, M., Sprague, S., Johnson-Masotti, A. P. and Gafni, A. (2005). An economic analysis of management strategies for closed and open grade I tibial shaft fractures. *Acta Orthop* **76**, 705–712.

Calve, S., Odelberg, S. J. and Simon, H.-G. (2010). A transitional extracellular matrix instructs cell behavior during muscle regeneration. *Dev Biol* **344**, 259–271.

Campbell, J. T. and Kaplan, F. S. (1992). The role of morphogens in endochondral ossification. *Calcif Tissue Int* **50**, 283–289.

Chandler, R. L., Chandler, K. J., McFarland, K. A. and Mortlock, D. P. (2007). Bmp2 transcription in osteoblast progenitors is regulated by a distant 3' enhancer located 156.3 kilobases from the promoter. *Mol Cell Biol* **27**, 2934–2951.

Chevallier, A. and Kieny, M. (1982). On the role of the connective tissue in the patterning of the chick limb musculature. *Wilhelm Roux' Archiv* **191**, 277–280.

Chevallier, A., Kieny, M. and Mauger, A. (1977). Limb-somite relationship: origin of the limb musculature. *J Embryol Exp Morphol* **41**, 245–258.

Chi, J.-T., Rodriguez, E. H., Wang, Z., Nuyten, D. S. A., Mukherjee, S., van de Rijn, M., van de Vijver, M. J., Hastie, T. and Brown, P. O. (2007). Gene expression programs of human smooth muscle cells: tissue-specific differentiation and prognostic significance in breast cancers. *PLoS Genet* **3**, 1770–1784.

Chiquet, M. and Fambrough, D. M. (1984). Chick myotendinous antigen. I. A monoclonal antibody as a marker for tendon and muscle morphogenesis. *J. Cell Biol.* **98**, 1926–1936.

Chisaka, O. and Capecchi, M. R. (1991). Regionally restricted developmental defects resulting from targeted disruption of the mouse homeobox gene hox-1.5. *Nature* **350**, 473–479.

Christ, B., Jacob, H. J. and Jacob, M. (1977a). [Experimental findings on muscle development in the limbs of the chick embryo]. *Verh Anat Ges* 1231–1237.

Christ, B., Jacob, H. J. and Jacob, M. (1977b). Experimental analysis of the origin of the wing musculature in avian embryos. *Anat Embryol* **150**, 171–186.

Cohn, M. J., Patel, K., Krumlauf, R., Wilkinsont, D. G., Clarke, J. D. W. and Tickle, C. (1997). Hox9 genes and vertebrate limb specification. *Nature* **387**, 97–101.

Colnot, C., Huang, S. and Helms, J. (2006). Analyzing the cellular contribution of bone marrow to fracture healing using bone marrow transplantation in mice. *Biochem. Biophys. Res. Commun.* **350**, 557–561.

Colnot, C., Lu, C., Hu, D. and Helms, J. A. (2004). Distinguishing the contributions of the perichondrium, cartilage, and vascular endothelium to skeletal development. *Dev Biol* **269**, 55–69.

Condie, B. G. and Capecchi, M. R. (1994). Mice with targeted disruptions in the paralogous genes hoxa-3 and hoxd-3 reveal synergistic interactions. *Nature* **370**, 304–307.

Davis, A. P., Witte, D. P., Hsieh-Li, H. M., Potter, S. S. and Capecchi, M. R. (1995). Absence of radius and ulna in mice lacking hoxa-11 and hoxd-11. *Nature* **375**, 791–795.

Di Giacomo, G., Koss, M., Capellini, T. D., Brendolan, A., Pöpperl, H. and Selleri, L. (2006). Spatio-temporal expression of Pbx3 during mouse organogenesis. *Gene Expr Patterns* **6**, 747–757.

Dollé, P., Dierich, A., LeMeur, M., Schimmang, T., Schuhbaur, B., Chambon, P. and Duboule, D. (1993). Disruption of the Hoxd-13 gene induces localized heterochrony leading to mice with neotenic limbs. *Cell* **75**, 431–441.

Drosos, G. I. and Pozo, J. L. (2005). Large extrasynovial intracapsular ganglia of the knee: a report of 3 cases. *Arthroscopy* **21**, 1362–1365.

Edom-Vovard, F., Schuler, B., Bonnin, M.-A., Teillet, M.-A. and Duprez, D. (2002). Fgf4 positively regulates scleraxis and tenascin expression in chick limb tendons. *Dev Biol* **247**, 351–366.

Eloy-Trinquet, S., Wang, H., Edom-Vovard, F. and Duprez, D. (2009). Fgf signaling components are associated with muscles and tendons during limb development. *Dev Dyn* **238**, 1195–1206.

Ferguson, C., Alpern, E., Miclau, T. and Helms, J. A. (1999). Does adult fracture repair recapitulate embryonic skeletal formation? *Mech Dev* **87**, 57–66.

Fromental-Ramain, C., Warot, X., Lakkaraju, S., Favier, B., Haack, H., Birling, C., Dierich, A., Doll e, P. and Chambon, P. (1996a). Specific and redundant functions of the paralogous Hoxa-9 and Hoxd-9 genes in forelimb and axial skeleton patterning. *Development* **122**, 461–472.

Fromental-Ramain, C., Warot, X., Messadecq, N., LeMeur, M., Dollé, P. and

Chambon, P. (1996b). Hoxa-13 and Hoxd-13 play a crucial role in the patterning of the limb autopod. *Development* **122**, 2997–3011.

Gersch, R. P., Lombardo, F., McGovern, S. C. and Hadjiargyrou, M. (2005). Reactivation of Hox gene expression during bone regeneration. *J Orthop Res* **23**, 882–890.

Gerstenfeld, L. C., Cullinane, D. M., Barnes, G. L., Graves, D. T. and Einhorn, T. A. (2003). Fracture healing as a post-natal developmental process: molecular, spatial, and temporal aspects of its regulation. *J Cell Biochem* **88**, 873–884.

Gesta, S., Blüher, M., Yamamoto, Y., Norris, A. W., Berndt, J., Kralisch, S., Boucher, J., Lewis, C. and Kahn, C. R. (2006). Evidence for a role of developmental genes in the origin of obesity and body fat distribution. *Proc Natl Acad Sci USA* **103**, 6676–6681.

Gilbert, S. F. and Knisely, K. *Developmental Biology 9th Ed*. Sinauer Associates Incorporated.

Grim, M. and Wachtler, F. (1991). Muscle morphogenesis in the absence of myogenic cells. *Anat Embryol* **183**, 67–70.

Haack, H. and Gruss, P. (1993). The establishment of murine Hox-1 expression domains during patterning of the limb. *Dev Biol* **157**, 410–422.

Hall, B. K. and Herring, S. W. (1990). Paralysis and growth of the musculoskeletal system in the embryonic chick. *J. Morphol.* **206**, 45–56.

Hankenson, K. D., Dishowitz, M., Gray, C. and Schenker, M. (2011). Angiogenesis in bone regeneration. *Injury* **42**, 556–561.

Hasson, P., DeLaurier, A., Bennett, M., Grigorieva, E., Naiche, L. A., Papaioannou, V. E., Mohun, T. J. and Logan, M. P. O. (2010). ScienceDirect - Developmental Cell : Tbx4 and Tbx5 Acting in Connective Tissue Are Required for Limb Muscle and Tendon Patterning. *Dev Cell* **18**, 148–156.

Henrotin, Y. (2011). Muscle: a source of progenitor cells for bone fracture healing. *BMC Med* **9**, 136.

Hiltunen, A., Vuorio, E. and Aro, H. T. (1993). A standardized experimental fracture in the mouse tibia. *J Orthop Res* **11**, 305–312.

Horan, G. S., Ramírez-Solis, R., Featherstone, M. S., Wolgemuth, D. J., Bradley, A. and Behringer, R. R. (1995). Compound mutants for the paralogous hoxa-4, hoxb-4, and hoxd-4 genes show more complete homeotic transformations and a dose-dependent increase in the number of vertebrae transformed. *Genes Dev* **9**, 1667–1677.

Hosseini, A. and Hogg, D. A. (1991). The effects of paralysis on skeletal development in the chick embryo. I. General effects. *J Anat* **177**, 159–168.

Hostikka, S. and Capecchi, M. R. (1998). The mouse Hoxc11 gene: genomic structure and expression pattern. *Mech Dev*.

Hsieh-Li, H. M., Witte, D. P., Weinstein, M., Branford, W., Li, H., Small, K. and Potter, S. S. (1995). Hoxa 11 structure, extensive antisense transcription, and function in male and female fertility. *Development* **121**, 1373–1385.

Huppert, S. S., Ilagan, M. X. G., De Strooper, B. and Kopan, R. (2005). Analysis of Notch function in presomitic mesoderm suggests a gamma-secretase-independent role for presenilins in somite differentiation. *Dev Cell* **8**, 677–688.

Ito, Y., Fitzsimmons, J. S., Sanyal, A., Mello, M. A., Mukherjee, N. and O'Driscoll, S. W. (2001). Localization of chondrocyte precursors in periosteum. *Osteoarthr. Cartil.* **9**, 215–223.

Izpisúa-Belmonte, J. C. and Duboule, D. (1992). Homeobox genes and pattern formation in the vertebrate limb. *Dev Biol* **152**, 26–36.

Jacob, M., Christ, B. and Jacob, H. J. (1979). The migration of myogenic cells from the somites into the leg region of avian embryos. An ultrastructural study. *Anat Embryol* **157**, 291–309.

Jones, E. and Yang, X. (2011). Mesenchymal stem cells and bone regeneration: current status. *Injury* **42**, 562–568.

Kaplan, F. S. and Shore, E. M. (1996). Bone morphogenetic proteins and C-FOS: early signals in endochondral bone formation. *Bone* **19**, 13S–21S.

Kardon, G. (1998). Muscle and tendon morphogenesis in the avian hind limb. *Development*.

Kardon, G., Campbell, J. K. and Tabin, C. J. (2002). Local extrinsic signals determine muscle and endothelial cell fate and patterning in the vertebrate limb. *Dev Cell* **3**, 533–545.

Kardon, G., Harfe, B. D. and Tabin, C. J. (2003). A Tcf4-positive mesodermal population provides a prepattern for vertebrate limb muscle patterning. *Dev Cell* **5**, 937–944.

Karsenty, G. (2008). Transcriptional control of skeletogenesis. *Annu Rev Genomics Hum Genet* **9**, 183–196.

Karsenty, G., Kronenberg, H. M. and Settembre, C. (2009). Genetic control of bone formation. *Annu. Rev. Cell Dev. Biol.* **25**, 629–648.

Kaufman, T. C., Seeger, M. A. and Olsen, G. (1990). Molecular and genetic organization of the antennapedia gene complex of Drosophila melanogaster. *Adv. Genet.* **27**, 309–362.

Khosla, S. and Eghbali-Fatourechi, G. Z. (2006). Circulating cells with osteogenic potential. *Ann N Y Acad Sci* **1068**, 489–497.

Khosla, S., Westendorf, J. J. and Mödder, U. I. (2010). Concise review: Insights from normal bone remodeling and stem cell-based therapies for bone repair. *Stem Cells* **28**, 2124–2128.

Kieny, M. and Chevallier, A. (1979). Autonomy of tendon development in the embryonic chick wing. *J Embryol Exp Morphol* **49**, 153–165.

Kmita, M., Tarchini, B., Zakany, J., Logan, M., Tabin, C. J. and Duboule, D. (2005). Early developmental arrest of mammalian limbs lacking HoxA/HoxD gene function. *Nature* **435**, 1113–1116.

Kohrs, R. T., Zhao, C., Sun, Y.-L., Jay, G. D., Zhang, L., Warman, M. L., An, K.-N. and Amadio, P. C. (2011). Tendon fascicle gliding in wild type, heterozygous, and lubricin knockout mice. *J Orthop Res* **29**, 384–389.

Komori, T., Yagi, H., Nomura, S. and Yamaguchi, A. (1997). ScienceDirect.com - Cell - Targeted Disruption of Cbfa1Results in a Complete Lack of Bone Formation owing to Maturational Arrest of Osteoblasts. *Cell*.

Kronenberg, H. M. (2007). The role of the perichondrium in fetal bone development. *Ann N Y Acad Sci* **1116**, 59–64.

Krumlauf, R. (1994). Hox genes in vertebrate development. *Cell* **78**, 191–201.

Leucht, P., Kim, J.-B., Amasha, R., James, A. W., Girod, S. and Helms, J. A. (2008). Embryonic origin and Hox status determine progenitor cell fate during adult bone regeneration. *Development* **135**, 2845–2854.

Lewis, E. B. (1963). Genes and Developmental Pathways. *jstor.org* **3**, 33–56.

Lewis, E. B. (1978). A gene complex controlling segmentation in Drosophila. *Nature* **276**, 565–570.

Lewis, E. B. (1985). Regulation of the genes of the bithorax complex in Drosophila. *Cold Spring Harb. Symp. Quant. Biol.* **50**, 155–164.

Maes, C., Kobayashi, T., Selig, M. K., Torrekens, S., Roth, S. I., Mackem, S., Carmeliet, G. and Kronenberg, H. M. (2010). ScienceDirect.com - Developmental Cell - Osteoblast Precursors, but Not Mature Osteoblasts, Move into Developing and Fractured Bones along with Invading Blood Vessels. *Dev*

Cell **19**, 329–344.

Malizos, K. N. and Papatheodorou, L. K. (2005). The healing potential of the periosteum molecular aspects. *Injury* **36 Suppl 3**, S13–9.

Mallo, M., Vinagre, T. and Carapuço, M. (2009). The road to the vertebral formula. *Int J Dev Biol* **53**, 1469–1481.

Mallo, M., Wellik, D. M. and Deschamps, J. (2010). Hox genes and regional patterning of the vertebrate body plan. *Dev Biol* **344**, 7–15.

Mathew, S. J., Hansen, J. M., Merrell, A. J., Murphy, M. M., Lawson, J. A., Hutcheson, D. A., Hansen, M. S., Angus-Hill, M. and Kardon, G. (2011). Connective tissue fibroblasts and Tcf4 regulate myogenesis. *Development* **138**, 371–384.

Matsumoto, T., Kuroda, R., Mifune, Y., Kawamoto, A., Shoji, T., Miwa, M., Asahara, T. and Kurosaka, M. (2008). Circulating endothelial/skeletal progenitor cells for bone regeneration and healing. *Bone* **43**, 434–439.

McIntyre, D. C., Rakshit, S., Yallowitz, A. R., Loken, L., Jeannotte, L., Capecchi, M. R. and Wellik, D. M. (2007). Hox patterning of the vertebrate rib cage. *Development* **134**, 2981–2989.

Mehrotra, M., Williams, C. R., Ogawa, M. and Larue, A. C. (2012). Hematopoietic stem cells give rise to osteo-chondrogenic cells. *Blood Cells Mol. Dis.*

Mendelsohn, C., Batourina, E., Fung, S., Gilbert, T. and Dodd, J. (1999). Stromal cells mediate retinoid-dependent functions essential for renal development. *Development* **126**, 1139–1148.

Mortlock, D. P. (2003). A General Approach for Identifying Distant Regulatory Elements Applied to the Gdf6 Gene. *Genome Research* **13**, 2069–2081.

Murchison, N. D., Price, B. A., Conner, D. A., Keene, D. R., Olson, E. N., Tabin, C. J. and Schweitzer, R. (2007). Regulation of tendon differentiation by scleraxis distinguishes force-transmitting tendons from muscle-anchoring tendons. *Development* **134**, 2697–2708.

Nakahara, H., Bruder, S. P., Haynesworth, S. E., Holecek, J. J., Baber, M. A., Goldberg, V. M. and Caplan, A. I. (1990). Bone and cartilage formation in diffusion chambers by subcultured cells derived from the periosteum. *Bone* **11**, 181–188.

Nakashima, K., Zhou, X., Kunkel, G., Zhang, Z., Deng, J. M., Behringer, R. R. and de Crombrugghe, B. (2002). ScienceDirect.com - Cell - The Novel Zinc Finger-Containing Transcription Factor Osterix Is Required for Osteoblast

Differentiation and Bone Formation. *Cell* **108**, 17–29.

Nelson, L. T., Rakshit, S., Sun, H. and Wellik, D. M. (2008). Generation and expression of a Hoxa11eGFP targeted allele in mice. *Dev Dyn* **237**, 3410–3416.

Oni, O. O., Hui, A. and Gregg, P. J. (1988). The healing of closed tibial shaft fractures. The natural history of union with closed treatment. *J Bone Joint Surg Br* **70**, 787–790.

Ordahl, C. P. and Le Douarin, N. M. (1992). Two myogenic lineages within the developing somite. *Development* **114**, 339–353.

Otto, F., Thornell, A. P., Crompton, T., Denzel, A., Gilmour, K. C., Rosewell, I. R., Stamp, G. W. H., Beddington, R. S. P., Mundlos, S., Olsen, B. R., et al. (1997). Cbfa1, a Candidate Gene for Cleidocranial Dysplasia Syndrome, Is Essential for Osteoblast Differentiation and Bone Development. *Cell* **89**, 765–771.

Park, D., Spencer, J. A., Koh, B. I., Kobayashi, T., Fujisaki, J., Clemens, T. L., Lin, C. P., Kronenberg, H. M. and Scadden, D. T. (2012). ScienceDirect.com - Cell Stem Cell - Endogenous Bone Marrow MSCs Are Dynamic, Fate-Restricted Participants in Bone Maintenance and Regeneration. *Cell Stem Cell* **10**, 259–272.

Pathi, S., Rutenberg, J. B., Johnson, R. L. and Vortkamp, A. (1999). Interaction of Ihh and BMP/Noggin signaling during cartilage differentiation. *Dev Biol* **209**, 239–253.

Pearson, J. C., Lemons, D. and McGinnis, W. (2005). Modulating Hox gene functions during animal body patterning. *Nat Rev Genet* **6**, 893–904.

Puchtler, H., Waldrop, F. S. and Valentine, L. S. (1973). Polarization Microscopic Studies of Connective Tissue Stained with Picro-Sirius Red FBA. *Beiträge zur Pathologie* **150**, 174–187.

Rinn, J. L., Bondre, C., Gladstone, H. B., Brown, P. O. and Chang, H. Y. (2006). Anatomic demarcation by positional variation in fibroblast gene expression programs. *PLoS Genet* **2**, e119.

Rinn, J. L., Wang, J. K., Allen, N., Brugmann, S. A., Mikels, A. J., Liu, H., Ridky, T. W., Stadler, H. S., Nusse, R., Helms, J. A., et al. (2008). A dermal HOX transcriptional program regulates site-specific epidermal fate. *Genes Dev* **22**, 303–307.

Rodriguez-Guzman, M., Montero, J. A., Santesteban, E., Gañan, Y., Macias, D. and Hurle, J. M. (2007). Tendon-muscle crosstalk controls muscle bellies morphogenesis, which is mediated by cell death and retinoic acid signaling. *Dev Biol* **302**, 267–280.

Rong, P. M., Teillet, M. A., Ziller, C. and Le Douarin, N. M. (1992). The neural tube/notochord complex is necessary for vertebral but not limb and body wall striated muscle differentiation. *Development* **115**, 657–672.

Rumi, M. N., Deol, G. S., Singapuri, K. P. and Pellegrini, V. D. (2005). The origin of osteoprogenitor cells responsible for heterotopic ossification following hip surgery: an animal model in the rabbit. *J Orthop Res* **23**, 34–40.

Schindeler, A., McDonald, M. M., Bokko, P. and Little, D. G. (2008). Bone remodeling during fracture repair: The cellular picture. *Semin Cell Dev Biol* **19**, 459–466.

Schneider, C. A., Rasband, W. S. and Eliceiri, K. W. (2012). NIH Image to ImageJ: 25 years of image analysis. *Nat Methods* **9**, 671–675.

Schneuwly, S., Klemenz, R. and Gehring, W. J. (1987). Redesigning the body plan of Drosophila by ectopic expression of the homoeotic gene Antennapedia. *Nature* **325**, 816–818.

Schweitzer, R., Chyung, J. H., Murtaugh, L. C., Brent, A. E., Rosen, V., Olson, E. N., Lassar, A. and Tabin, C. J. (2001). Analysis of the tendon cell fate using Scleraxis, a specific marker for tendons and ligaments. *Development* **128**, 3855–3866.

Scott, M. P. (1992). Vertebrate homeobox gene nomenclature. *Cell* **71**, 551–553.

Small, K. M. and Potter, S. S. (1993). Homeotic transformations and limb defects in Hox A11 mutant mice. *Genes Dev* **7**, 2318–2328.

Stadler, H. S., Higgins, K. M. and Capecchi, M. R. (2001). Loss of Eph-receptor expression correlates with loss of cell adhesion and chondrogenic capacity in Hoxa13 mutant limbs. *Development* **128**, 4177–4188.

Staverosky, J. A., Pryce, B. A., Watson, S. S. and Schweitzer, R. (2009). Tubulin polymerization-promoting protein family member 3, Tppp3, is a specific marker of the differentiating tendon sheath and synovial joints. *Dev Dyn* **238**, 685–692.

Svingen, T. and Tonissen, K. F. (2006). Hox transcription factors and their elusive mammalian gene targets. *Heredity (Edinb)* **97**, 88–96.

Sweat, F., Puchtler, H. and Rosenthal, S. I. (1964). Sirius red F3BA as a stain for connective tissue. *Arch Pathol* **78**, 69–72.

Swinehart, I. T., Schlientz, A. J., Quintanilla, C. A., Mortlock, D. P. and Wellik, D. M. *Hox11 function is required regionally for the patterning and integration of muscle, tendon and bone*.

Tamer, El, M. K. and Reis, R. L. (2009). Progenitor and stem cells for bone and cartilage regeneration. *J Tissue Eng Regen Med* **3**, 327–337.

Thompson, Z., Miclau, T., Hu, D. and Helms, J. A. (2002). A model for intramembranous ossification during fracture healing. *J Orthop Res* **20**, 1091–1098.

Tozer, S. and Duprez, D. (2005). Tendon and ligament: development, repair and disease. *Birth Defects Res. C Embryo Today* **75**, 226–236.

Tozer, S., Bonnin, M.-A., Relaix, F., Di Savino, S., García-Villalba, P., Coumailleau, P. and Duprez, D. (2007). Involvement of vessels and PDGFB in muscle splitting during chick limb development. *Development* **134**, 2579–2591.

Ushiku, C., Adams, D. J., Jiang, X., Wang, L. and Rowe, D. W. (2010). Long bone fracture repair in mice harboring GFP reporters for cells within the osteoblastic lineage. *J Orthop Res* **28**, 1338–1347.

van den Akker, E., Fromental-Ramain, C., de Graaff, W., Le Mouellic, H., Brûlet, P., Chambon, P. and Deschamps, J. (2001). Axial skeletal patterning in mice lacking all paralogous group 8 Hox genes. *Development* **128**, 1911–1921.

Väänänen, H. K. and Laitala-Leinonen, T. (2008). Osteoclast lineage and function. *Arch. Biochem. Biophys.* **473**, 132–138.

Vortkamp, A., Pathi, S., Peretti, G. M., Caruso, E. M., Zaleske, D. J. and Tabin, C. J. (1998). Recapitulation of signals regulating embryonic bone formation during postnatal growth and in fracture repair. *Mech Dev* **71**, 65–76.

Wachtler, F., Christ, B. and Jacob, H. J. (1981). On the determination of mesodermal tissues in the avian embryonic wing bud. *Anat Embryol* **161**, 283–289.

Wang, J. H.-C., Guo, Q. and Li, B. (2012). Tendon biomechanics and mechanobiology--a minireview of basic concepts and recent advancements. *J Hand Ther* **25**, 133–40– quiz 141.

Wellik, D. M. (2007). Hox patterning of the vertebrate axial skeleton. *Dev Dyn* **236**, 2454–2463.

Wellik, D. M. and Capecchi, M. R. (2003). Hox10 and Hox11 genes are required to globally pattern the mammalian skeleton. *Science* **301**, 363–367.

Wellik, D. M., Hawkes, P. J. and Capecchi, M. R. (2002). Hox11 paralogous genes are essential for metanephric kidney induction. *Genes Dev* **16**, 1423–1432.

Xu, B. and Wellik, D. M. (2011). Axial Hox9 activity establishes the posterior field in

the developing forelimb. *Proc Natl Acad Sci USA* **108**, 4888–4891.

Xu, B., Takeuchi, J. K., McIntyre, D. C., Wellik, D., Novitch, B. G., Jeannotte, L. and Gaber, Z. B. (submitted). *Hox5 paralogous genes interact with Plzf to define the forelimb anterior domain by repressing Shh*.

Zakany, J. and Duboule, D. (2007). The role of Hox genes during vertebrate limb development. *Curr. Opin. Genet. Dev.* **17**, 359–366.

Zakany, J., Zacchetti, G. and Duboule, D. (2007). Interactions between HOXD and Gli3 genes control the limb apical ectodermal ridge via Fgf10. *Dev Biol* **306**, 883–893.

Zimmermann, G., Schmeckenbecher, K. H. K., Boeuf, S., Weiss, S., Bock, R., Moghaddam, A. and Richter, W. (2012). Differential gene expression analysis in fracture callus of patients with regular and failed bone healing. *Injury* **43**, 347–356.